

Evaluation of Roadway Concrete Barriers and Materials

Vista Shahriari, M.S.
Pavana Prabhakar, Ph.D.
Jose A. Pincheira, Ph.D.

University of Wisconsin – Madison
Department of Civil and Environmental Engineering

WisDOT ID no. 0092-19-03

July 2021



RESEARCH & LIBRARY UNIT



WISCONSIN HIGHWAY RESEARCH PROGRAM

WISCONSIN DOT
PUTTING RESEARCH TO WORK

Disclaimer

This research was funded through the Wisconsin Highway Research Program by the Wisconsin Department of Transportation and the Federal Highway Administration under Project 0092-19-03. The contents of this report reflect the views of the authors who are responsible for the facts and accuracy of the data presented herein. The contents do not necessarily reflect the official views of the Wisconsin Department of Transportation or the Federal Highway Administration at the time of publication.

This document is disseminated under the sponsorship of the Department of Transportation in the interest of information exchange. The United States Government assumes no liability for its contents or use thereof. This report does not constitute a standard, specification or regulation.

The United States Government does not endorse products or manufacturers. Trade and manufacturers' names appear in this report only because they are considered essential to the object of the document.

TECHNICAL REPORT DOCUMENTATION PAGE

1. Report No. WHRP 0092-19-03	2. Government Accession No.	3. Recipient's Catalog No.	
4. Title and Subtitle Evaluation of Roadway Concrete Barriers and Materials		5. Report Date July 2021	
		6. Performing Organization Code	
7. Author(s) Vista Shahriari, Pavana Prabhakar, Jose A. Pincheira		8. Performing Organization Report No.	
9. Performing Organization Name and Address University of Wisconsin – Madison Department of Civil and Environmental Engineering 2205 Engineering Hall 1415 Engineering Dr. Madison, WI 53706		10. Work Unit No.	
		11. Contract or Grant No. WHRP 0092-19-03	
12. Sponsoring Agency Name and Address Wisconsin Department of Transportation Research & Library Unit 4822 Madison Yards Way Room 911 Madison, WI 53705		13. Type of Report and Period Covered Final Report October 2018 – July 2021	
		14. Sponsoring Agency Code	
15. Supplementary Notes			
16. Abstract The research objective was to investigate the causes and sources of distress observed in single-slope slip-formed roadway concrete barriers with the goal of developing strategies to ensure the long-term performance of these barriers in Wisconsin. To that end, barriers built between 2012 and 2015 and located in three different regions of WI were studied. The research approach included a state-wide survey, field inspection of the barriers, as well as laboratory tests of concrete cores and powder samples. Data analysis was performed to distinguish between observed types and the extent of distress. Based on the findings, several recommendations are presented which include improving construction practices, inspection, and quality control during construction, following concrete specification, improving data collection during barrier construction, limiting the size of aggregates, modifications to the amount of horizontal reinforcement, and heat of hydration of cement.			
17. Key Words Single-slope Barriers; Distress; Non-Destructive Evaluation; Mechanical Testing		18. Distribution Statement No restrictions. This document is available through the National Technical Information Service. 5285 Port Royal Road Springfield, VA 22161	
19. Security Classif. (of this report) Unclassified	20. Security Classif. (of this page) Unclassified	21. No. of Pages 66	22. Price

Form DOT F 1700.7 (8-72)

Reproduction of completed page authorized

Executive Summary

Single-slope slip-formed concrete barriers that have been in service for several years (many since 2011) are deteriorating at an advanced rate in the state of Wisconsin. Hence, the Wisconsin Department of Transportation (WisDOT) has identified a need to investigate the sources of distress observed in single-slope roadway concrete barriers that may significantly reduce their service life. Examples of barrier distresses include vertical and horizontal cracks, map cracking, and spalling. In addition to the added maintenance or replacement costs associated with reduced barrier durability, early deterioration may reduce the capacity and crash performance of the barrier, thus increasing the probability of a fatality. There are several factors that may affect the durability of concrete barriers, which include (a) composition and quality of the concrete, (b) the level of exposure to deicing solutions, (c) the stresses induced by volume changes due to shrinkage or temperature variations and (d) the construction procedure. To that end, the main purpose of this investigation is to conduct an in-depth study for identifying sources and causes of distress that affect the performance of barriers in WI, and propose recommendations for improving their long-term performance. Four concrete barriers across different regions of Wisconsin and construction year ranges from 2012 - 2015 were selected for this purpose. One of the visited barriers was located in the NWR (NW-1 in Eau Claire county), two in the SE (SE-1 and SE-2 in Milwaukee county), and one in the SWR (SW-1 in Dane county) of WI.

The research approach primarily included conducting: 1) a review of the types of concrete mix design, quality control documents, and construction methods, 2) a state-wide survey to identify the commonly observed types of distress, 3) field inspections to characterize and assess the extent of damage of the most common types of distress, and 4) laboratory examinations of core and powder samples to validate field observations. The field study included several methods to assess the current condition of the barriers, the rebar layout, as well as the overall health of the concrete and rebar. The methods used in the field inspection were: 1) Visual Inspection (VI), 2) Ground Penetrating Radar (GPR), 3) Ultrasonic Pulse Velocity (UPV), and 4) Half-Cell Potential (HCP). The field study was complemented with core and powder extraction in addition to evaluation of the condition of concrete and of the exposed bars after coring. The laboratory examinations included: 1) Core examination, 2) Carbonation depth, 3) Water absorption, 4) Ultrasonic Pulse Velocity (UPV), 5) Chloride ion content, 6) Compressive strength, Alkali-Silica Reaction, and 7) CT scan imaging.

Discussion of key findings, observations and recommendations of this research is as follows:

- The type of distress observed in the barriers investigated was confined primarily to the presence of vertical cracks throughout the length of the inspected segments. Minor concrete spalling along both or one of the faces of the cracks was observed over a short length in some cases. This spalling, however, was not observed to be widespread. All barriers inspected in this study showed vertical cracks that varied in spacing, width, and length. Vertical cracks that extended over the barrier height were generally wider and extended through the thickness of the barrier. The shorter vertical cracks near the bottom do not appear to extend through the thickness, though this could not be verified in all cases because of backfill in some of the barriers. Barrier SE-2 showed in addition horizontal cracks near the top of the barrier as well as random cracks in all directions (map cracking) in between vertical cracks.
- There are no universally agreed values of acceptable maximum crack widths. Traditionally, however, cracks wider than 0.016 in. are considered unsightly and can lead to public concern. Furthermore, cracks in exposed surfaces, as is the case of barriers, will be more noticeable due to streaks of dirt and percolated chemicals or liquids. Other than an unsightly appearance, the observed crack widths in barriers NW-1 and SE-1 do not appear to be of concern in terms of structural integrity. On the other hand, the extent (number and size) of cracking observed in barriers SE-2 and SW-1 may be considered to affect the structural integrity of the barrier and should be avoided. The amount of concrete cover is important to control the width of surface cracks. Many of the bars in the barriers studied were placed with a side cover much larger, up to ~ 2 times of their specified value of 2 inches. For example, with a cover of 4 inches, the crack widths would increase by about 20 percent. It is recognized that the standard tolerances used in common reinforced concrete construction (beams, slabs, and columns) are difficult to follow in slip-form construction of the barriers; however, every effort should be made to adhere to the specified concrete cover to control the widths of the cracks in the barriers.
- Accurate prediction of the number, size, and spacing of cracks in reinforced concrete members is, in general, a difficult task. The problem is further compounded in the case of shrinkage cracking, because of the uncertainty in predicting shrinkage strains, even under controlled environmental conditions in the laboratory. The crack spacing was estimated using the recommendations of the CEB-FIB Code while the crack width was estimated using the well-known equation proposed by Gergely and Lutz. To provide a range of expected values, the

spacing and crack widths were computed for steel stress of $0.67f_y$ (lower bound) and $1.0f_y$ (upper bound), where f_y is the yield stress of the reinforcement, taken as 60 ksi. The calculations show that the average spacing between vertical cracks varies slightly with barrier type, but it is expected to be about 1.7 ft. This value is in line with the observed spacing of the large vertical cracks in all barriers, except in barrier NW-1 where the spacing of 3 - 4 ft was observed.

- As mentioned above, barrier SE-2 showed map cracking in addition to vertical cracks. The most common causes for these cracks are: (a) expansion due to alkali-silica reaction (ASR); (b) surface drying shrinkage restrained by the underlying concrete; and (c) restrained thermal contraction, particularly at early ages of the concrete.

Results from the ASR tests were negative, indicating no signs of ASR in the concrete used in these barriers. Therefore, ASR is not considered a plausible source of the observed cracks in barrier SE-2 or in any of the other barriers investigated.

Map cracking due to surface drying shrinkage cracks or due to thermal expansion are nearly impossible to prevent, but they can be reduced by following careful construction and curing procedures. Drying shrinkage cracks can be minimized by avoiding the surface to dry before starting curing procedures; therefore, curing of the barrier should begin as soon as possible after finishing.

To control cracks due to restrained thermal contraction, the temperature and heat during cement hydration must be controlled. Standard procedures to minimize concrete temperature and heat include reducing the cement content and/or cooling of the concrete. It is noted that the cement content used in barrier SE-2 was much higher (480 lbs./yd³) than the specified value for A-FA grade concrete (395 lb./yd³), which points at one of the plausible reasons for the excessive number and size of the cracks observed for this barrier.

- If a wall (the barrier in this case) is cast on a foundation cast sometime before, shrinkage is restrained by the foundation as the early barrier concrete cools down to ambient temperatures. This gives rise to a heat-of-hydration cracking pattern consisting of large widely spaced cracks extending from the bottom to the top of the member, with some shorter vertical cracks extending from the bottom, a crack pattern that is similar to that observed in the barriers investigated in this study. Heat-of-hydration cracks can be controlled by controlling the heat rise due to heat of hydration, by placing the members in short lengths, or by providing reinforcement in excess of the normal shrinkage reinforcement. It is noted that as much as three

times the normal shrinkage reinforcement may be required to limit shrinkage cracks to reasonable widths. The reinforcement ratio provided in barrier types S32 and S42 of this study is 0.0041 and 0.0043, respectively. This amount is about 2.2 times the standard shrinkage reinforcement. Therefore, while reinforcement in excess of the standard shrinkage reinforcement has been specified and provided in these barriers, it may not be sufficient to limit cracking to reasonable widths.

- The ambient conditions (ambient temperature, humidity, high or low winds) existing at the time of construction of the barriers investigated were not recorded and it is unknown. Also, the exact season when these barriers were constructed was not recorded. Whether standard measures to control the heat of hydration (use of insulating blankets, for example) were used in the field during construction is unknown. Therefore, it is not possible to assert whether high levels of heat of hydration contributed to the excessive cracking observed in barrier SE-2, but because of the higher cement content used in this barrier it remains as a plausible explanation.
- The data from GPR and from UPV measurements taken over the inspected barrier lengths did not show indications of voids or poor consolidation to suggest widespread deterioration of stiffness or strength of the concrete. Locally, however, cores extracted from barrier SE-2 showed evidence of voids and poor consolidation in this barrier. This is further evidence that the concrete used in this barrier was of substandard quality.
- The source or type of aggregates used in the barriers, either crushed limestone or riverbed gravel, cannot be considered, per se, to influence the performance of the barriers. However, two contrasting characteristics were identified for the aggregates used in the barriers studied: size and distribution. The quality of the concrete with crushed, mostly smaller ($< \frac{3}{4}$ in) uniformly distributed gradation was in better condition than that containing large (up to 2 inches) poorly distributed coarse aggregates. Barriers in poorer condition (SE-1) had in fact what might be referred to as a gap-graded distribution with very large coarse gravel and only a few particles of smaller size aggregate. The large coarse aggregate used in barriers (SE-1) likely reduced workability and consolidation of the concrete. A more uniform gradation is expected to improve concrete strength, stiffness, workability, and long-term durability. Therefore, gap-graded, with large aggregate size (say > 1.5 inches) should be avoided.

Summary of Recommendations

- Control heat of hydration:
 - Use low heat of hydration cement or admixture to lower the heat of hydration which will reduce the likelihood of developing restrained shrinkage cracks.
 - Curing should begin as soon as possible after finishing.
 - Use insulating blankets to maintain the difference between internal and external temperature to 30 F or less.
- Aggregate size/distribution use well-graded coarse aggregates with coarse aggregate size no bigger than $\frac{3}{4}$ inch. Avoid gap-graded gradation with large coarse aggregate size.
- Increasing the amount of reinforcement to about 0.005-0.0055 seems prudent. This amount corresponds to the recommended amount to control restrained shrinkage in cases of severe cracking such as those observed in barrier SE-2.
- The tolerances for bar placement (spacing and concrete cover) must be tightened and every effort should be made to conform to standard tolerances used in reinforced concrete structures.
- Data collection during and after construction should be improved. This will assist researchers in future investigations like the present study:

During construction: recording curing procedures, ambient temperature during the concreting, additional procedures followed due to cold or hot weather, slump, air content, concrete class, exact aggregate, and cement type and source for each barrier segment, aggregate gradation, aggregate properties such as specific gravity and absorption, in addition to recording separate cylinder test reports for concrete barriers (i.e. not as part of ancillary items) would be recommended. Also, documenting the concrete specified mix design which includes all the mix materials with the amount, type and manufacturer, air content, slump, and water to cement ratio would be beneficial. After construction: performing regular inspection (yearly) to record the deterioration index with photos would help with cost analysis in future studies.
- Improving inspection and quality control during construction should ensure higher quality concrete. This could include ensuring that the cement content follows the specified value (395 lb./yd³). Likewise, ensuring a sufficient number of test cylinders as per the requirement for class I concrete (provided in QMP 715) will help monitor and track the quality of the placed concrete.

Table of Contents

Disclaimer	ii
Executive Summary	iv
Summary of Recommendations	viii
List of Figures	xii
List of Tables	xiv
Chapter 1 Introduction	15
1.1 Background	15
1.2 Research Objectives	16
1.3 Research Scope	16
Chapter 2 Literature Review	18
2.1 Introduction	18
2.2 Previous Studies on Concrete Barriers	18
Chapter 3 Barrier Selection Criteria for Field Inspections	20
3.1 Overview	20
3.2 Summary of Results	20
Chapter 4 Design Specifications and Test Records	23
4.1 Introduction	23
4.2 Summary and Discussion	23
Chapter 5 Field Inspection Procedures	28
5.1 Introduction	28
5.2 Visual Inspection (VI)	28
5.3 Ground Penetrating Radar (GPR) Imaging	28
5.4 Ultrasonic Pulse Velocity (UPV) Test	29
5.5 Half-Cell Potential (HCP)	30

5.6 Infrared (IR) Thermography	31
5.7 Core Extraction	31
5.8 Chloride Ion Concrete Powder Extraction	32
Chapter 6 Laboratory Test Procedures	34
6.1 Introduction.....	34
6.2 Core Examination	34
6.3 Carbonation Depth Measurement	34
6.4 Water Absorption Measurement	35
6.5 Ultrasonic Pulse Velocity (UPV) Measurement on Cores.....	36
6.6 Chloride Ion Penetration Measurement	36
6.7 Compressive Strength Measurement	36
6.8 Alkali-Silica Reaction (ASR) Detection.....	37
6.9 CT Scan Imaging	38
Chapter 7 Field Inspections – Summary of Results and Discussion	39
7.1 Introduction.....	39
7.2 Summary and Discussion.....	39
7.2.1 Visual Inspection	39
7.2.2 Half-Cell Potential (HCP) Measurements	42
7.2.3 Ground penetrating radar (GPR).....	43
7.2.4 Ultrasonic Pulse Velocity (UPV).....	46
Chapter 8 Laboratory Tests - Summary of Results and Discussion	47
8.1 Introduction.....	47
8.2 Summary and Discussion.....	47
8.2.1 Coarse Aggregate Size and Distribution.....	47
8.2.2 Carbonation Depth.....	51

8.2.3 Water Absorption.....	51
8.2.4 Ultrasonic Pulse Velocity (UPV).....	52
8.2.5 Chloride Ion Content.....	52
8.2.6 Compressive Strength	54
Chapter 9 Conclusions and Recommendations.....	55
9.1 Summary	55
9.2 Main Findings	55
9.2.1 Findings from the State-Wide Survey (Chapter 3)	55
9.2.2 Findings from Documents Provided by WisDOT (Chapter 4)	55
9.2.3 Findings from Field Inspections (Chapter 7).....	56
9.2.4 Findings from Laboratory Tests (Chapter 8).....	57
9.3 Conclusions.....	57
9.4 Analysis and Discussion of Results	58
9.5 Summary of Recommendations	62
References.....	64
Appendices.....	66

List of Figures

Figure 3.1: Typical section for single-slope concrete barriers type S32 and S42 [Adapted from Ref. [9] (see Table 3-1 for the dimensions A, B, and H, number of bars, and side cover)	21
Figure 4.1: Compressive strength based on the cylinder test results vs the specified value (notes: 1) at site SE-1, west (W) and east (E) segments were poured on different days, 2) one cylinder test data was available for the east segment, and 3) cylinder test data are provided by WisDOT).....	23
Figure 4.2: Measured air content based on the cylinder test reports and quality control documents vs specified range (note: at site SE-1, west (W) and east (E) segments were poured in different months)	24
Figure 5.1: a) GSSI StructureScan™ Mini XT unit [25], b) GSSI StructureScan™ Mini HR unit [26].....	28
Figure 5.2: Ultrasonic Pulse Velocity (UPV) test set-up.....	29
Figure 5.3: Procedure to find the epoxy-coated rebar and connect the electrode to it	30
Figure 5.4: Half-Cell Potential (HCP) test set-up.....	31
Figure 5.5: Set-up for core extraction.....	32
Figure 5.6: Concrete powder extraction procedure in the field: a) cleaning the hole, b) extracting powder sample, and c) collected samples	33
Figure 6.1: Carbonation depth test set-up and presentation of one sample before and after applying Phenolphthalein solution.....	35
Figure 6.2: Directions of UPV test performance on the extracted cores: a) axial, b) radial.....	36
Figure 6.3: Compression test set-up.....	37
Figure 6.4: Alkali-silica reaction (ASR) detection kit.....	37
Figure 6.5: A sample of ASR gel detection procedure on SER extracted core: a) freshly cut surface, b) after application of distilled water, c) after application of yellow reagent, d) after application of pink reagent.....	38
Figure 7.1: Typical crack patterns observed at each site	41
Figure 7.2: Half-cell potential readings along one longitudinal rebar at each site	42
Figure 7.3: Gray scale image of vertical GPR scans obtained along the barrier height: a) site NW-1 and b) site SE-1(W)	44
Figure 7.4: Average measured side concrete cover at different sites based on the GPR data	45

Figure 7.5: Average measured rebar spacing at different sites based on the GPR data	45
Figure 8.1: Samples of CT scan images of each site: a) site NW-1, b) site SE-1, c) site SE-2, d) site SW-1.....	49
Figure 8.2: Level of honeycombing in the extracted cores: a) SE-2 (the most distressed barrier), b) NW-1 (the least distressed barrier).....	50
Figure 8.3: Coarse aggregate greater than the specified dimension at site SE-1: a) longitudinal view, b) cross-section view.....	50
Figure 8.4: Total volume of permeable pore space (%).....	51
Figure 8.5: Measured chloride ion content of the extracted concrete samples at 0.5 inches to 1-inch depth (note: there was no construction joint at this sites NW-1 and SW-1).....	53
Figure 8.6: Measured compressive strength of the concrete.....	54

List of Tables

Table 3-1: Barrier section properties for S32 and S42 [9](note: see Figure 3.1 for the barrier parameters).....	21
Table 3-2: Summary of final selected barrier stretches for field inspection.....	22
Table 3-3: Site visited date and direction	22
Table 4-1: Construction month of visited sites based on cylinder test reports	25
Table 4-2: Aggregate source of visited sites.....	25
Table 4-3: Cement type and source of each site based on the cylinder test reports and the specified mix design.....	26
Table 4-4: Recorded slump as per available cylinder test reports vs the specified value [14], [17], [21].....	26
Table 4-5: A summary used cement, fly ash, and admixtures at each site based on the available cylinder test reports.....	26
Table 4-6: A summary of compressive strength evaluation of class II and I concrete as per 2017 revision of QMP 716 and 715 [23], [24].....	27
Table 5-1: Number of cores extracted per visited site	32
Table 7-1: Summary of observed distress and deterioration in inspected barriers	40
Table 7-2: Barrier ranking based on the observed condition the field.....	40
Table 7-3: Calculated average crack spacing and crack widths	40
Table 7-4: Length and condition of barrier visited	41
Table 7-5: Measured cover of the top layer of reinforcement	46
Table 8-1: Cross-section of the extracted cores	48
Table 8-2: Visual appearance of the barrier vs the average large aggregate distribution at one cross-section of extracted cores and aggregate type.....	49
Table 8-3: Effect of air void content on chloride ion content.....	53

Chapter 1 Introduction

1.1 Background

Over the past several years, Jersey type concrete barriers have been the most popular type of roadway concrete barriers. However, the primary disadvantage of this type was a need to be maintained each time a new layer of pavement was overlaid. The new layer of pavement decreased the height, changed the shape, and influenced the effectiveness of the Jersey barrier. Therefore, a new design was developed to solve these problems by constructing a taller barrier with only a single slope [1]. By using single-slope barriers, pavements could be overlaid without any significant effect on the height and shape of the barriers. They also can be constructed with the slip-formed technique rather than the cast-in-place method.

Even though the new design solved the above-described problems, it has been observed in Wisconsin that some of these single-slope slip-formed concrete barriers are deteriorating at an advanced rate which may significantly reduce their service life. Examples of barrier distress that have been reported include transverse (vertical), longitudinal (horizontal), and map cracking. In addition to the extra maintenance or replacement costs associated with reduced barrier durability, early deterioration may reduce the capacity and crash performance of the barrier which could lead to an increase in the probability of a fatality. Therefore, there is a need to investigate the sources of distress observed in single-slope slip-formed roadway concrete barriers.

There are several factors that may affect the durability of concrete barriers. Some of these factors include (a) composition and quality of the concrete, (b) the level of exposure to deicing solutions (e.g., deicing entrapment due to snow-build up), (c) the stresses induced by volume changes due to shrinkage or temperature variations, and (d) the construction procedure (form-cast or slip-formed).

Past studies have shown that the performance of concrete barriers depends on many factors, some of which have been outlined above. The present study focuses on identifying the sources and causes of distress that affect the performance (crash performance of the barrier is not included in this study) of concrete barriers in Wisconsin by conducting (a) a review of the types of concrete mix design, quality control documents, and construction methods, (b) a state-wide survey to identify the commonly observed types of distress, (c) field inspections to characterize and assess

the extent of damage of the most common types of distress, and (d) laboratory examinations of core samples to corroborate and validate field observations. Based on the results of this study, recommendations for improving the long-term performance of concrete barriers are provided.

1.2 Research Objectives

The broad objectives of this research are: 1) to determine and characterize the main types of concrete distress observed in single-slope concrete barriers; 2) to investigate the causes and sources of distress in these barriers and suggest strategies to prevent them; 3) to update the current Wisconsin Department of Transportation (WisDOT) barrier practices such as concrete barrier design, construction method, and maintenance procedures to ensure long-term performance of the barriers. In particular, the following questions/concerns are addressed as part of the research conducted within this project:

- What are the barrier designs, construction methodologies, and inspection procedures currently used in Wisconsin? How do they compare against other DOTs in the country?
- How robust are the materials used in single-slope concrete barriers installed in Wisconsin?
- What strategies can be adopted for improving the design, construction, and materials used in concrete barrier construction?

The above questions are addressed to achieve the objectives through a review of existing literature, field observations, and measurements coupled with laboratory experimental studies. The findings from the current study are condensed into a series of recommendations targeted at concrete traffic barrier designers and contractors in order to minimize any potential barrier distress.

1.3 Research Scope

The scope of this study includes reviewing concrete mix design, quality control documents, as-built drawings, etc. of the visited single-slope concrete barriers across Wisconsin, a state-wide survey, field, and laboratory measurements to assess the distress condition of these barriers.

A survey was sent to the WisDOT regional offices to gather information on the common types of distress (i.e. vertical, horizontal, map cracking, pop-outs, etc.), frequency of occurrence (i.e. very common, common, rarely, or never), construction season of the barriers, and some other information that were helped ascertain the potential sources of damage.

Two locations in the NW region, two in the SE region, and one in the SW region were selected to conduct field and laboratory tests. The total length of the visited barriers was about 1500 feet. Field studies include several non-destructive techniques which were visual inspection (VI) to evaluate the field and laboratory test results, infrared (IR) thermography imaging to detect near-surface damages and cracks, ground penetrating radar (GPR) imaging to evaluate internal deterioration, and estimate rebar spacing and cover, ultrasonic pulse velocity (UPV) test to evaluate internal flaws and determine material properties, and half-cell potential (HCP) measurement to determine the level of rebars corrosion activity. Laboratory tests include determination of chloride ion content over height and depth of barriers, carbonation depth, compressive strength, water absorption, alkali-silica reaction (ASR) detection, UPV, and CT scan imaging conducted on the cores extracted.

Field and laboratory data were analyzed, the corresponding documents of each visited barrier such as concrete mix design and quality control were studied and the results were cross-correlated to investigate the sources and causes of distresses observed in the barriers. In addition, recommendations for improving the design, construction, and materials used in concrete barrier construction are proposed. Some avenues to enhance the durability and treatment of concrete barriers from common distresses observed are also provided in this report.

Chapter 2 Literature Review

2.1 Introduction

In this chapter, a summary of some previous observations and experiences regarding the study of roadway concrete barriers and their proposed methods of investigation are presented.

2.2 Previous Studies on Concrete Barriers

There are several research projects from different states and regions of the United States which studied roadway concrete barriers and explored the application of different non-destructive evaluation techniques to assess the in-situ barrier conditions. The results of these studies were used to compare construction techniques and methodologies used nation-wide with observed performance. The type and severity of distress observed in Wisconsin with that in other states were of particular interest. A summary of a few of the most relevant studies is presented next, which were selected from regions with similar environmental conditions and demands as Wisconsin.

A study from Iowa and Illinois [2] focused on performing different non-destructive evaluations on concrete barriers to detect and assess distress types. In other words, this study evaluated several non-destructive evaluation techniques that could be effective in detecting anomalies in concrete barriers, such as corrosion and internal defects. This project developed guidelines for evaluating these barriers.

In a report from North Dakota [3], the use of Texcote XL-70C bridge cote as a concrete surface finish and curing compound was studied. The scope of the study was to determine if this coating could be a durable surface finish for the concrete barriers in the long-term. The results showed that the application of XL-70C was difficult and further research would be needed to determine its performance as a surface finish.

Two reports from Michigan were reviewed as part of the current study. In one report [4] the authors suggested that early barrier deterioration was initiated primarily by the formation of full or partial-depth vertical cracks. These cracks were attributed to the stresses arising from non-uniform shrinkage and thermal strains due to the restraint at the road-barrier interface. This study also reported observations of continuous longitudinal cracking and staining approximately four inches below the top surface (commonly seen in slip-formed barriers). These cracks were believed to

occur as the concrete in the upper portion of the barrier (top four inches) was supported by the top longitudinal reinforcement and restrained from the settlement, while the lower mass of concrete slumped downward under its own weight. Other types of distresses commonly observed included map cracking, spalling, delamination, pop-outs, efflorescence, and corrosion of reinforcement.

One of the main scopes of this study was also to determine potential factors of this premature deterioration of concrete barriers. Eventually, several recommendations were proposed to increase the service life of Portland cement concrete median barrier in Michigan, such as discontinuing the use of blast-furnace slag and other highly absorptive coarse aggregates, specifying at least seven days of wet curing for all the newly constructed barriers, and exploring the option of protective coatings or sealers on the surface of concrete barriers against deicer attack. In addition, discontinuing the slip-formed construction was suggested because this method exposed the fresh concrete surface to severe shrinkage stress when drying at an early age. The other report from Michigan [5] studied the causes and cures for cracking of concrete barriers. The main goal of this research was to develop techniques for decreasing the amount of premature distresses which formed as vertical cracks due to early-age thermal loading. There were several recommendations as a result of this study, such as using crack arrestors and modifying concrete mix design to generate lower heat of hydration and provide curing tolerable concrete. This study also suggested delaying the curing process to five to seven days after the placement of form-cast barriers.

In a study from Oregon [6] which focused on the concrete barrier distress in La Grande, the main reason for vertical cracks in that region was determined as exposure to freezing and thawing during cold seasons. This study concluded that using adequate entrained air volume could decrease the severity of distress due to freeze and thaw conditions.

As per the previous studies on roadway concrete barriers, the application of Texcote XL-70C as a concrete surface finish and curing compound was not easy. Vertical cracks are the common early-age distress observed which occur due to non-uniform shrinkage and thermal strains. To decrease this level of deterioration, discontinuing the slip-formed method, performing proper curing procedure, modifying the concrete mix, having sufficient entrained air, and exploring the option of the protective coating were proposed. In the current study, some of the proposed NDE techniques in the literature review with several additional ones and laboratory tests were used to investigate the sources and causes of distresses observed in concrete barriers across Wisconsin.

Chapter 3 Barrier Selection Criteria for Field Inspections

3.1 Overview

In this study, the following steps were used to select the locations of the barriers for field inspections. A summary of the results is presented here, and the detailed approach is provided in Appendix B.

1. Review of existing barriers in WI: According to the database, most single-slope barriers have been constructed mainly since 2009. Thus, barriers built prior to this date were not considered further in this study. The total length of single-slope barriers built since 2009 is almost 300 miles which are distributed in about 200 locations across WI.
2. State-Wide Survey of WI Regions: The research team at the University of Wisconsin – Madison designed a state-wide survey which was reviewed and distributed by the POC members of the Wisconsin Department of Transportation (WisDOT). The main goal of this survey was to identify commonly observed types of barrier distresses in each region of Wisconsin. Details such as the list of questions, respondents' answers, and analysis of the results are provided in Appendix C.
3. Summary of Results from Steps 1 and 2
4. Expected Crack Pattern: An estimation for the expected vertical cracking (i.e. crack width and spacing) using CEB-FIP (International Federation for Structural Concrete) recommendations [7] and Gergely – Lutz equation [8] were provided. This estimation could help in evaluating the severity of distress by comparing it to the expected amount.
5. Selection of Barriers for Field Inspection

3.2 Summary of Results

Based on a review of the existing barriers in WI, the results of the state-wide survey, and discussion with the project oversight committee (POC) members, the following conclusions were derived:

1. Because each region uses its local aggregate source, it would be reasonable to visit locations that use different aggregates.
2. It would be helpful to visit the locations with the least and most amount of distress to compare and investigate the reasons for highly damaged barriers.

3. The visited sites were either S32 or S42 [9] type barrier. The detailed layout of these types of barriers according to the as-built drawings of this project is shown in Figure 3.1 with corresponding parameters shown in Table 3-1.
4. By comparing the types and levels of distress in addition to the construction year of the proposed barriers in the NW, SE, and SW region of Wisconsin by POC, five locations were selected for field inspection. A summary of selected locations for a field visit for performing the non-destructive evaluations and core extraction as well as the reasons for this selection are provided in Table 3-2. Table 3-3 shows the date of visit for each site and the direction in which the field inspection was performed.

A complete description and details of the barriers selected for study including location, year of construction, project ID, and as-built drawings are provided in Appendix D.

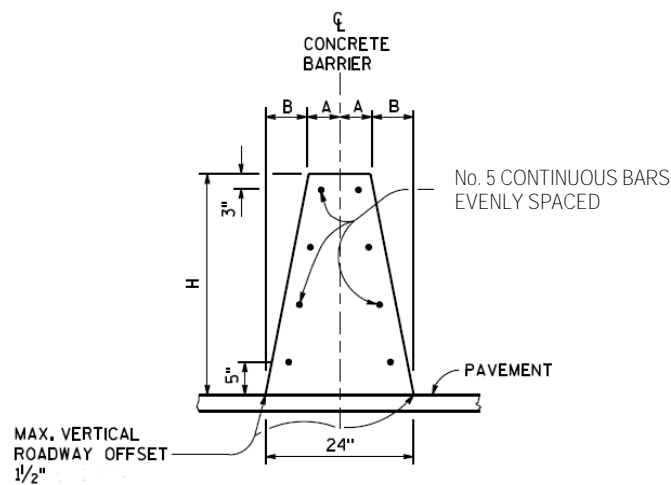


Figure 3.1: Typical section for single-slope concrete barriers type S32 and S42 [Adapted from Ref. [9] (see Table 3-1 for the dimensions A, B, and H, number of bars, and side cover)

Table 3-1: Barrier section properties for S32 and S42 [9](note: see Figure 3.1 for the barrier parameters)

Barrier type	H (in)	A (in)	B (in)	Number of no.5 bars	Specified clear side cover (in)
S32	32	7	5	8	2
S42	42	5 ¼	6 ¾	10	2

Table 3-2: Summary of final selected barrier stretches for field inspection

Site (barrier type) ⁺	Project ID	Project year	County	Route number	Reason for selection
NW-1 (S42)	1022-08-73	2013	Eau Claire	I 94	A different source of aggregate and built-year as compared with other sites. Different levels of distress as compared with site SE-2 even though the built-year is only one year different.
NW-2* (N/A)	1020-06-72	1996	Eau Claire	I 94	Different levels of distress as compared with site NW-1 even though they are in the same county.
SE-1 (S42)	1060-33-80	2015	Milwaukee	I 94	A different source of aggregate and built-year as compared with other sites. Unexpected vertical cracks are reported even though it is the newest barrier among all the selected ones.
SE-2 (S32)	1030-20-72	2012	Milwaukee	I 94	A different source of aggregate and built-year as compared with other sites. Unexpected map cracking is reported even though it is built only a year before site NW-1.
SW-1 (S42)	5300-04-77	2014	Dane	US 12	A different source of aggregate and built-year as compared with other sites. Less distress is reported than site SE-1 even though site SE-1 is built a year after this site.

*Site NW-2 was reported as a single-slope slip-formed barrier with the same project ID and built year as site NW-1. However, after the site visit, it seemed that the barrier was older, not single-slope, and was constructed in segments rather than slip-formed. Thus, data regarding this site is not considered in this study.

+Barrier section properties for each type are shown in Table 3-1.

Table 3-3: Site visited date and direction

Site	Date visited	Direction
NW-1	5/29/2019	Westbound – Right Lane Shoulder
NW-2	5/29/2019	Westbound – Left Lane Median
SE-1	6/20/2019	Westbound – Right Lane Shoulder
SE-2	6/21/2019	Northbound – Left Lane Median
SW-1	10/30/2019	Westbound – Right Lane Shoulder

Chapter 4 Design Specifications and Test Records

4.1 Introduction

In this chapter, a summary of the comparison of several barrier characteristics among the visited sites is presented based on the existing data, such as the results of cylinders cast closest to the barriers visited, concrete mix design, and quality control documents.

4.2 Summary and Discussion

By comparing the compressive strength of the barriers as per the cylinder test reports cast closest to the segment visited at each site ([10]–[13]) with the specified value, it can be seen site SE-2 is the only one with compressive strength less than the specified value (Figure 4.1). This site was the most distressed one among all the visited barriers. On the other hand, site NW-1 which was in the relatively best condition compared with the other sites shows a compressive strength of about 50% higher than the specified value. It is worth noting that due to lack of information regarding the specified compressive strength value of each site, they were all assumed similar to the available value for site SE-2 (i.e. 4500 psi [14]).

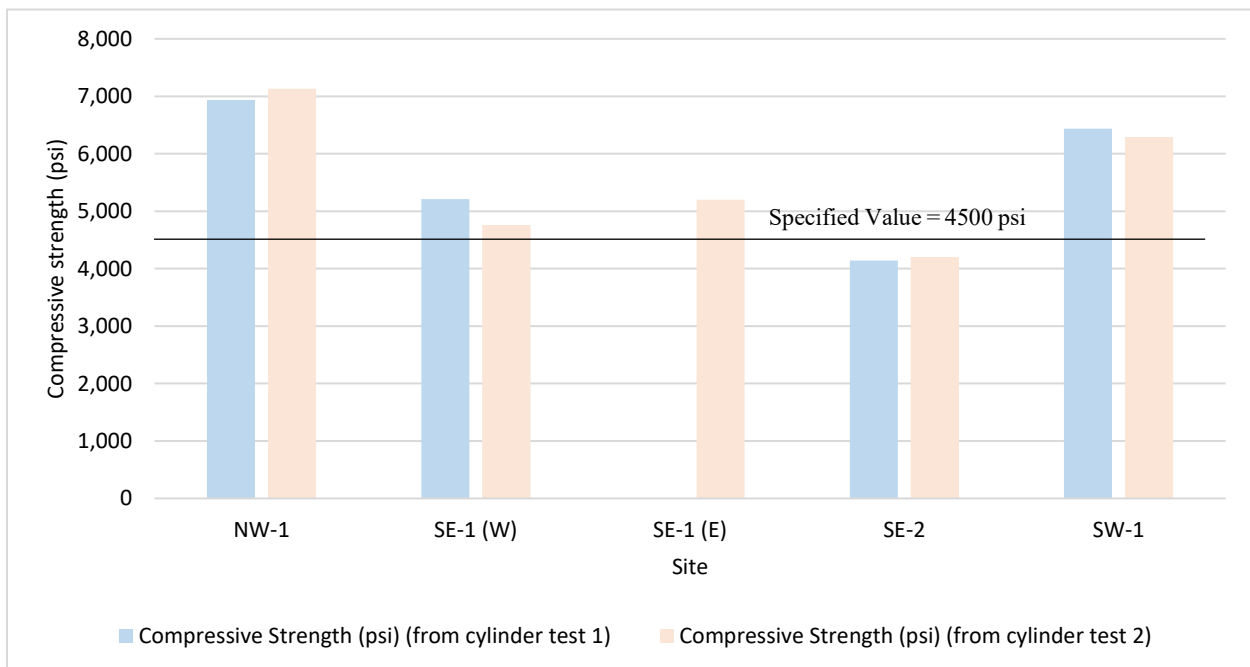


Figure 4.1: Compressive strength based on the cylinder test results vs the specified value (notes: 1) at site SE-1, west (W) and east (E) segments were poured on different days, 2) one cylinder test data was available for the east segment, and 3) cylinder test data are provided by WisDOT)

In addition, comparing the manufacturer of concrete admixtures among the visited sites (Appendix D) shows that sites NW-1 and SW-1 used General Resource Technology admixtures, while sites SE-1 and SE-2 used Sika Corporation products. All the added admixtures were in the approved products list provided by WisDOT [15].

Furthermore, by looking at the measured air content which is provided in quality control documents or cylinder test reports ([10]–[13]) of the visited sites, and comparing them with the specified range (i.e. 5.5% to 8.5% [16]), it can be seen all the air contents are in the specified range in (Figure 4.2). However, site SE-1 (E) is in the very low range.

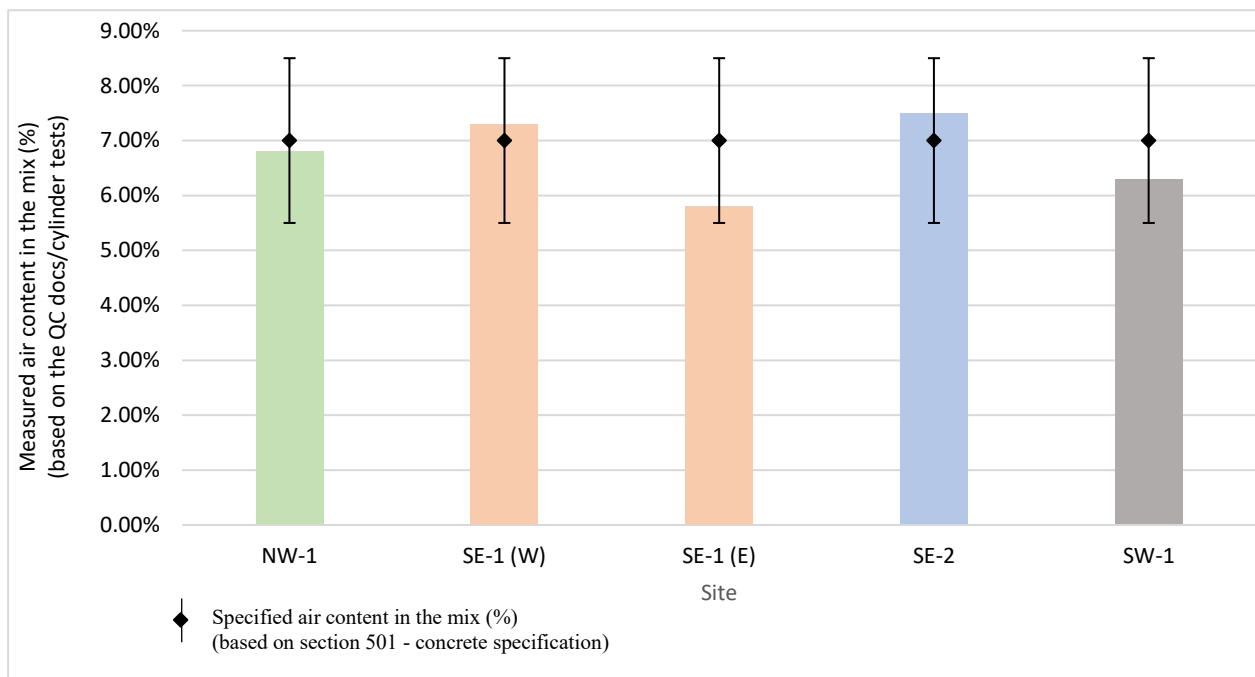


Figure 4.2: Measured air content based on the cylinder test reports and quality control documents vs specified range (note: at site SE-1, west (W) and east (E) segments were poured in different months)

Based on the available cylinder test reports ([10]–[13]), the month of construction was also compared among the visited barriers (Table 4-1). Here, the sampling date in the provided cylinder test reports was assumed as a construction date. No trend was seen between the season of construction and the severity of distress in the visited sites.

Table 4-1: Construction month of visited sites based on cylinder test reports

Site	Construction month
NW-1	October
SE-1 (W)*	June
SE-1 (E)*	July
SE-2	September
SW-1	October

*At site SE-1, west (W) and east (E) segments were poured on different days.

In addition, based on the provided cylinder test reports ([10]–[13]) and communicating with the POC members, the most possible aggregate source was found for each visited site (Table 4-2). It shows none of the sites used the same source of aggregate to evaluate their quality among them.

Table 4-2: Aggregate source of visited sites

Site	Fine aggregate source	Coarse aggregate source
NW-1	AMERICAN MATERIALS #31 (Eau Claire)	MILESTONE MONDOVI (763) (Buffalo)
SE-1	LANNON (SUSSEX) (Waukesha)	LANNON (SUSSEX) (Waukesha)
SE-2	THELEN S & G (Lake Co., IL)	LAFARGE COLGATE (Waukesha)
SW-1	WINGRA (WEILAND-MARTY-PD) (Dane)	WINGRA (WEILAND-MARTY-PD) (Dane)

According to the available cylinder test reports and concrete mix design ([11]–[13], [17]), the cement type and source of each site are shown in Table 4-3. The results show using cement type II at site NW-1, with the barrier in the relatively best condition, while the other investigated sites used cement type I. Note that cement type II is low-alkali cement that could cause less alkali-silica reactivity in the concrete mix which leads to less cracking [18], [19].

In addition, sites NW-1 and SW-1 have “Holcim-St. Genevieve, MO” recorded as their cement source, whereas sites SE-1 and SE-2 have “St. Marys-Charlevoix, MI”. Two former sites were less distressed compared with the latter ones (i.e. less vertical cracks and no map cracking or horizontal cracks) as per visual inspection results in section 7.2.1.

Table 4-3: Cement type and source of each site based on the cylinder test reports and the specified mix design

Site	Cement type	Cement source
NW-1	II	Holcim-St. Genevieve, MO
SE-1	I	St. Marys-Charlevoix, MI
SE-2	I	St. Marys-Charlevoix, MI
SW-1	I	Holcim-St. Genevieve, MO

Furthermore, the recorded slump in cylinder test reports ([10]–[13]) as presented in Table 4-4 shows that concrete slump at site SE-2 was almost 2 times the specified value and 4 times the slump of the barrier at site NW-1. These reports also show that site SE-2 has the highest amount of cement in its mix among all the visited sites (Table 4-5). Excessive slump and cement content could be the contributors to the cracking of concrete at an early age [20].

Table 4-4: Recorded slump as per available cylinder test reports vs the specified value [14], [17], [21]

Site	Slump (in) as per cylinder test report	Specified slump (in)
NW-1	1.00	≤ 2.50 as per concrete pavement specification for slip-formed technique
SE-1	N/A ⁺	≤ 2.50 as per specified mix design
SE-2	3.75	½ of an inch to 2 inches as per specified mix design
SW-1	0.00	≤ 2.50 as per concrete pavement specification for slip-formed technique

⁺No data were available for the SE-1 barriers.

Table 4-5: A summary used cement, fly ash, and admixtures at each site based on the available cylinder test reports

Site	Cement (lbs.) ⁺⁺	Fly ash (lbs.) ⁺⁺	Air Entrainment (oz)	Water Reducer (oz)
NW-1	395	170	1.26	4.32
SE-1 (W)	398	171	10.00	23.10
SE-1 (E) ⁺	N/A	N/A	N/A	N/A
SE-2	480	135	11.50	18.8 and 12.00*
SW-1	394	170	3.01	4.31 and 2.86*

*Two water reducers were recorded in the cylinder test report. More details are provided in Appendix D.

⁺No data were available for the SE-1 (W) barrier.

⁺⁺A nominal cubic yard has the tabulated weights of cement and fly ash.

In addition, the requirements provided in the concrete mix design of site SE-1 [17] suggest the use of both class I and II concrete quality control plan at this site; however, the specified concrete class for the cast-in-place barriers was class II at the time of construction [22]. There are no data available for the other visited barriers. A summary of the difference between class I and II concrete in terms of compressive strength evaluation is summarized in Table 4-6.

Table 4-6: A summary of compressive strength evaluation of class II and I concrete as per 2017 revision of QMP 716 and 715 [23], [24]

Class II	Class I
<ul style="list-style-type: none"> - Cast one set of 2 cylinders per 200 cubic yards. 	<ul style="list-style-type: none"> - Use at least 5 pairs of cylinders. - Randomly select 2 QC cylinders as per QMP 715 requirements. - The department will evaluate the subplot for possible removal and replacement if the 28-day subplot average strength is lower than $f'c$ minus 500 psi. The value of $f'c$ is the design stress the plans show. The department may assess further strength price reductions or require removal and replacement only after coring the subplot. - If the 3-core average is greater than or equal to 85 percent of $f'c$, and no individual core is less than 75 percent of $f'c$, the engineer will accept the subplot at the previously determined pay for the lot. If the 3-core average is less than 85 percent of $f'c$, or an individual core is less than 75 percent of $f'c$, the engineer may require the contractor to remove and replace the subplot or assess a price reduction of \$35 per cubic yard or more.

Chapter 5 Field Inspection Procedures

5.1 Introduction

In this chapter, the field inspection techniques used at four sites with single-slope barriers in addition to test methods, general procedures, tools, and equipment are presented.

Non-destructive evaluation (NDE) techniques including Visual Inspection (VI), Ground Penetrating Radar (GPR) imaging, Ultrasonic Pulse Velocity (UPV) test, Half-Cell Potential (HCP) measurement, and Infrared (IR) Thermography were used to detect near-surface and in-depth anomalies of concrete barriers. In addition, core and concrete powder samples were extracted for physical examination and later testing in the laboratory. A description of the basic principles of the non-destructive methods used in the field are provided in Appendix A.

5.2 Visual Inspection (VI)

A detailed visual inspection of the concrete barriers was made at each site. The barriers dimensions were verified against those specified in the as-built plans, and photo logging and video recording were performed. A survey of the overall condition of the surface of the barriers was also conducted by documenting the presence of cracks, spalls, signs of corrosion (rust), and other signs of distress.

5.3 Ground Penetrating Radar (GPR) Imaging

A GSSI StructureScan™ Mini XT and Mini HR (Figure 5.1 [25], [26]) were used to perform GPR scanning in this study.



Figure 5.1: a) GSSI StructureScan™ Mini XT unit [25], b) GSSI StructureScan™ Mini HR unit [26]

The general protocol used for conducting the GPR scans was the same at all the site visits. It consisted of initial horizontal (and vertical) scanning of the barrier at different elevations to detect

any irregularities and distress inside of the concrete. These scans were mostly done in the areas with a larger number and wider cracks. It is worth noting that at some sites additional scans were performed in the areas with good conditions to investigate the dissimilarity.

Afterward, detailed vertical and horizontal scans using a 2 inches x 2 inches grid were conducted on a 2 ft x 2 ft surface area at two locations. At least one of these locations was within the area of the initial GPR scans. Details of the scanning procedures used at each site are described in Appendix E.

5.4 Ultrasonic Pulse Velocity (UPV) Test

Evaluation of the UPV method was performed using a PUNDIT Plus testing system with 55 kHz ultrasonic transducers, and a digital RIGOL DS1054z oscilloscope for real-time evaluation of ultrasonic waveforms through the concrete barriers. A water-based ultrasonic gel was used to establish the necessary acoustic coupling with the test surface.

UltraSigma and UltraScope software were installed to present and collect data for later analyses. Figure 5.2 shows the set-up for this test. At site NW-1, this test was conducted on the same regions where the detailed GPR grids were scanned, but with coarser grids. At SE sites UPV measurements could not be conducted due to the unexpected breakdown of the PUNDIT Plus equipment. Measurements at site SW-1 were conducted at a few points due to the simultaneous performance of the coring close to the UPV measurement section which caused noisy data. Details of this test procedure are described in Appendix E.

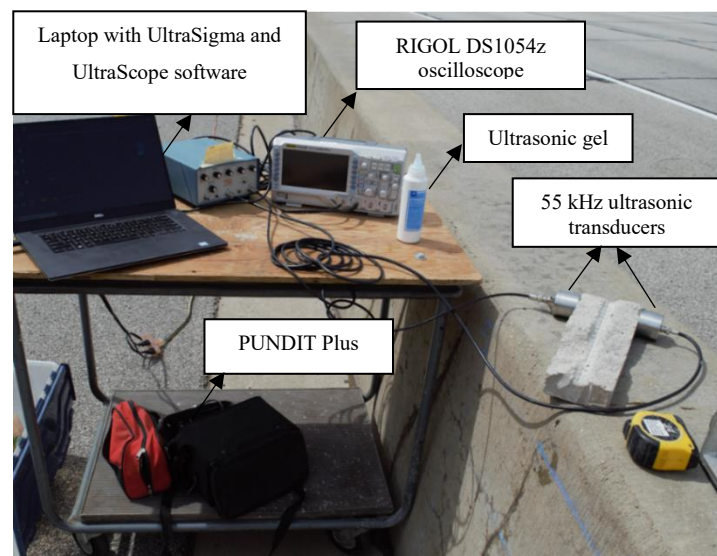


Figure 5.2: Ultrasonic Pulse Velocity (UPV) test set-up

5.5 Half-Cell Potential (HCP)

In this test, one connection to epoxy-coated rebar was used for each longitudinal line of readings. Pachometer, GPR, and as-built drawings of the projects were used to detect the approximate location of rebars inside the concrete barriers. Then, drilling was performed on a 3.6 inches diameter circle to get access to the epoxy-coated rebars (Figure 5.3). It is worth noting that the detection of rebar location with GPR scanning was within 1 inch of the actual location in all the visits.

To provide a proper connection to the rebars, it was decided to perform soldering. But the concrete cover was more than what was expected (i.e. it was supposed to be 2 inches as per SDD 14b32-a [9] while it was almost 4 inches) and soldering was not possible with the provided tools. Thus, the epoxy coating on the bars was completely removed with a Dremel rotary tool, and the electrode was clamped directly to the rebar.



Figure 5.3: Procedure to find the epoxy-coated rebar and connect the electrode to it

C-CM-4000 Cor-Map® System was used to conduct this test. It includes a reference electrode (i.e. solution of Cu/CuSo₄ crystals and distilled water) and electrode contact solution (i.e. solution of wetting agent and potable water) [27] which were made at each site to perform this test. A high impedance voltmeter was also used to read the potentials and a cable reel facilitated access to the farther points from the rebar connection. The set-up for this test is shown in Figure 5.4. The readings were made several points with 12 inches O.C. spacing at each site. Details of this test procedure at each site are described in Appendix E.

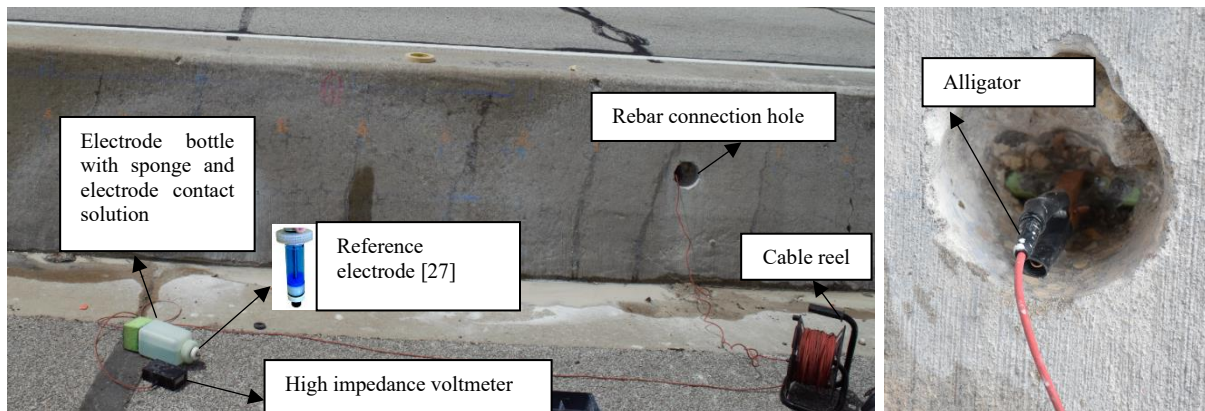


Figure 5.4: Half-Cell Potential (HCP) test set-up

5.6 Infrared (IR) Thermography

The Infrared thermography for this study was done with FLIR® E60 (details in Appendix E), which is capable of capturing details of thermal changes on external surfaces due to the presence of defects and distresses. According to ASTM D-4788-03 [28], getting meaningful results from infrared thermography requires several weather conditions, such as a minimum of 3 hours of direct sunshine, no rain for a minimum of 24 hours prior to the test, a rise of 20°F with 4 hours of sun, wind speed less than 15 mph (24 km/h) for Portland-cement concrete surfaces. Unfortunately, none of the sites visited satisfied most of the above-mentioned conditions. Therefore, this test was not performed in a meaningful way. Even though a few images were captured from the areas with cracks at site SE-2, they cannot be clearly interpreted.

5.7 Core Extraction

In this study, different sources of information were used to select the coring locations. GPR scans and visual inspections were the main sources that helped in this selection. GPR data detected the locations without the existence of rebar, while visual inspection showed the regions with near-surface anomalies, such as cracking, spalling, and delamination. To compare the quality and properties of concrete in the areas with good and poor conditions, 3.6 inches diameter core samples were extracted from areas with different levels of distress (i.e. cracks, spalling, etc.).

Coring was conducted in the areas between the longitudinal reinforcement layers. The length of cores varied between about 2 inches and 6 inches depending on the quality and strength of the concrete in each region. The stiffer the concrete, the harder it was to get a longer core. In addition, cores in the areas containing surface cracks were sometimes broken upon removal from the barrier. The typical set-up for core extraction is shown in Figure 5.5.



Figure 5.5: Set-up for core extraction

The cores were taken to the UW-Madison laboratory for more testing and analyses. They were also visually inspected to evaluate their overall condition, detect any distress, such as cracks, signs of corrosion, delamination, and study their aggregate size and type. Table 5-1 shows a summary of the total number of cores. The number of barrier segments at each visited site and the difference in the severity of distress along each segment were the major factors to decide the number of extracted cores. Core details corresponding to each site are presented in Appendix E.

Table 5-1: Number of cores extracted per visited site

Site	Number of extracted cores
NW-1	2
SE-1	2
SE-2	4
SW-1	3

5.8 Chloride Ion Concrete Powder Extraction

To perform the chloride ion test in the laboratory, concrete powder samples are required. Several powder samples were extracted during SE and SW field visits and brought to the UW-Madison laboratory. However, due to lack of time at some sites, the powder extraction was not conducted

on-site completely, and it was decided to retrieve powder samples in the laboratory from the extracted cores.

To perform concrete powder extraction at the site visits, a hammer drill was used with a 1-inch diameter bit to drill a pilot hole with approximately $\frac{1}{2}$ inches depth. The hole was cleaned with compressed air to remove all powder and debris. After cleaning the pilot hole, a smaller drill bit of $\frac{3}{4}$ inches diameter was used to drill an additional $\frac{1}{2}$ inches depth. The extracted material and powder from the depth of $\frac{1}{2}$ inches to 1-inch was collected in a container, sealed, and labeled. This method was repeated for different elevations and depths of the visited concrete barriers (Figure 5.6).

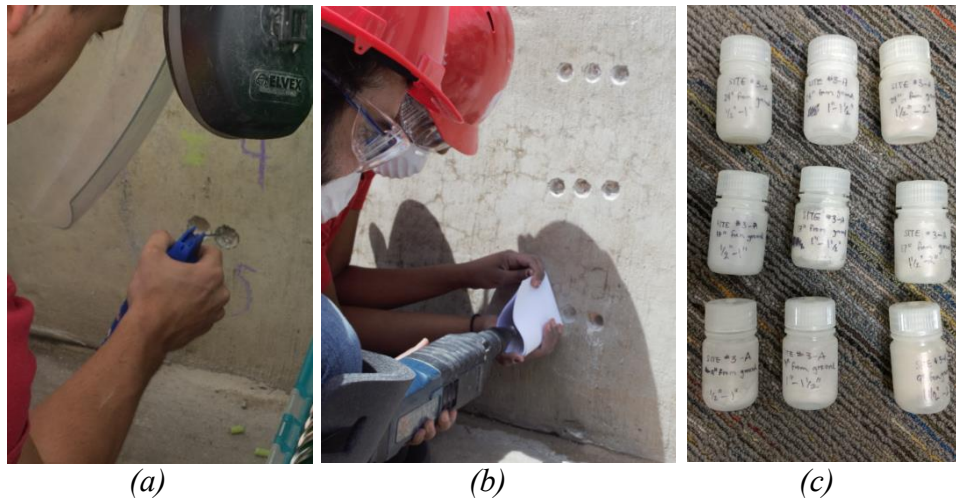


Figure 5.6: Concrete powder extraction procedure in the field: a) cleaning the hole, b) extracting powder sample, and c) collected samples

According to AASHTO T 260-97 (2011), a minimum of 10 grams of powder is needed to perform the chloride ion test. To collect this amount the research team had to drill more than one hole in some elevations to satisfy this AASHTO requirement. It is worth noting that all the equipment (i.e. drill bits and lab spatula) was cleaned with alcohol after drilling each hole and sample extraction to avoid cross-contamination between the samples. Details corresponding to each site are presented in Appendix E.

Chapter 6 Laboratory Test Procedures

6.1 Introduction

In this chapter, all the laboratory tests used on the extracted samples from four sites with single-slope barriers in addition to test methods, general procedures, tools, and equipment are presented.

During each visit concrete samples were extracted, labeled, and brought to the UW-Madison laboratory for more thorough investigations. This included the physical evaluation of the overall conditions of the cores, carbonation depth, water absorption, chloride ion penetration, and compressive strength measurement in addition to alkali-silica reaction (ASR) detection, UPV test on cores, and CT scan imaging. A description of the laboratory test methods is provided in Appendix A.

6.2 Core Examination

The extracted cores from each visited site were visually examined, photographed, and their measurements such as diameter, length, and mass were recorded. The diameter of each core was measured three times along the length of the core and the average value was used in calculation and data analysis. The length of each core was measured at four locations around the perimeter of the core to record the maximum and minimum values. The original mass value of each core was also measured before performing any tests.

In addition, the overall physical condition of each extracted core such as maximum and minimum size of the aggregates on the core surface, type of aggregates, and existence of cracking, sign of corrosion, and delamination were recorded.

6.3 Carbonation Depth Measurement

In this study, the recommendations of the RILEM CPC-18 [29] were used for the carbonation depth measurement of the extracted cores from each visited site. The test was done by cutting an approximately 0.25 inches slice of the extracted cores with a wet saw. One side of each slice was the exposed barrier surface. These slices were cut again in half to provide a suitable surface to conduct the test. After sawing, the broken surfaces were cleared immediately with a paper towel from loose particles and dried with a fan for less than a minute. Then the phenolphthalein solution

(i.e. 1% phenolphthalein in 70% ethyl alcohol) was sprayed on the broken surfaces. The set-up for this test and one sample before and after spraying the solution are shown in Figure 6.1.

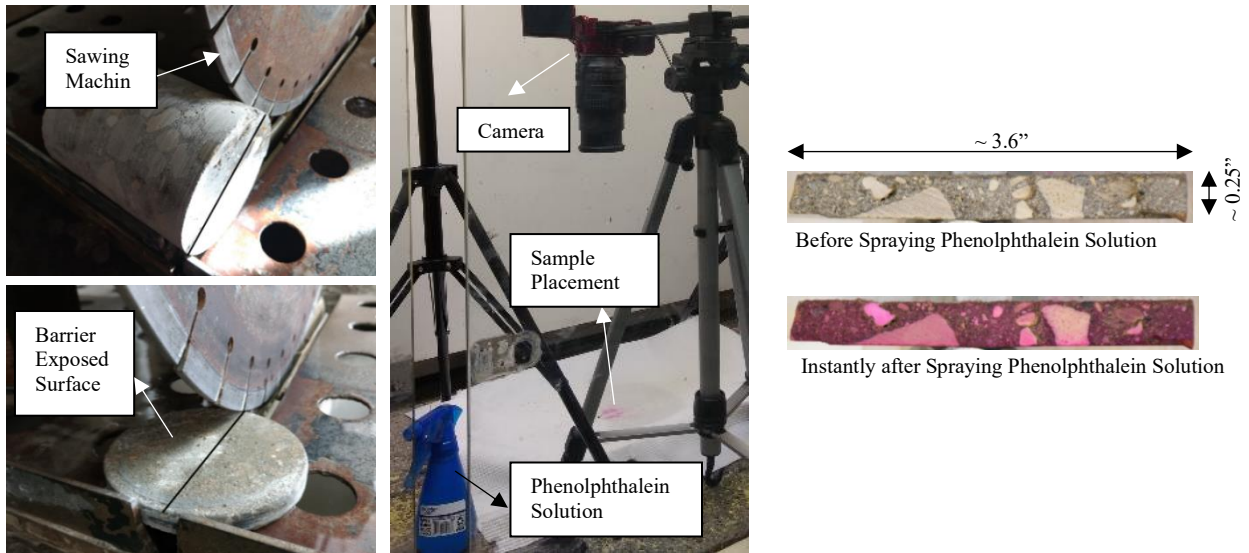


Figure 6.1: Carbonation depth test set-up and presentation of one sample before and after applying Phenolphthalein solution

The phenolphthalein solution reacts with the cement paste and leads to magenta color and colorless for non-carbonated and carbonated regions respectively. To enhance the contrast this solution was sprayed two times on each surface such that no flow channels formed, and photos were taken immediately to measure the carbonation depth. In addition, because the measured carbonation depth is affected by the time of measurement, all the sprayed samples are stored for 24 hours, and measurements were conducted again to have a better demonstration between carbonated and non-carbonated regions. Based on RILEM CPC-18 [29], when the sample had large aggregates the carbonation depth was measured where the hardened cement paste was predominant rather than where the aggregates were present.

6.4 Water Absorption Measurement

Based on ASTM C 642-13 [30], only the extracted cores with the minimum volume of 21.4 in^3 (350 cm^3) with no observable cracks or crushed edges could be used to perform the water absorption test. Thus, 9 out of 11 extracted cores from the visited sites in NW, SE, and SW regions were selected to conduct this test. In addition, based on the applied ASTM, the balance which was used in all steps of this test was sensitive to 0.025% of the values of core mass. The detailed procedure of this test is provided in Appendix F.

6.5 Ultrasonic Pulse Velocity (UPV) Measurement on Cores

To perform the UPV test on the extracted cores more precisely, two ends of each core were sawed to have flat surfaces for holding transducers. By eliminating the broken and very short cores, 9 cores were qualified to perform this test. These 9 cores were from all the visited sites with the single-slope barriers. The test was conducted in two directions, axial and radial, for each core to compare the results (Figure 6.2).

Same as UPV on-site, this test was performed using a PUNDIT Plus testing system with 55 kHz ultrasonic transducers, and a digital RIGOL DS1054z oscilloscope for real-time evaluation of ultrasonic waveforms through the concrete cores. A water-based ultrasonic gel was used to establish the necessary acoustic coupling with the test surface. UltraSigma and UltraScope software were used to present and collect data for analyses.

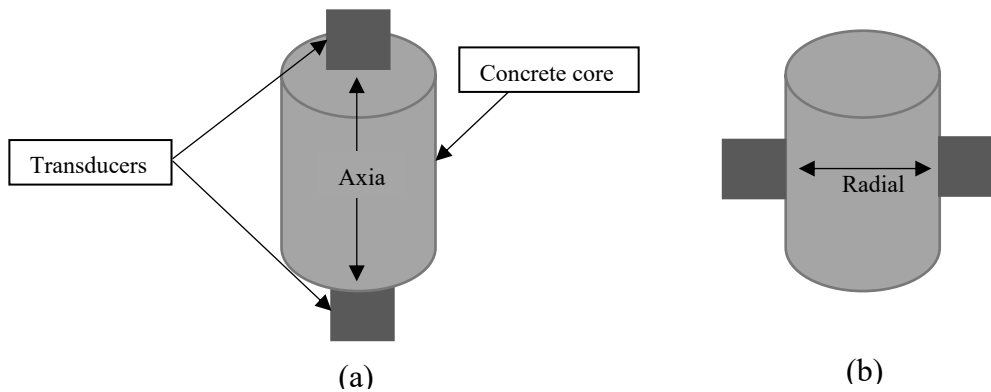


Figure 6.2: Directions of UPV test performance on the extracted cores: a) axial, b) radial

6.6 Chloride Ion Penetration Measurement

This was conducted in collaboration with Derek Sachs, a Master's student at the University of Wisconsin-Madison. The details of this test are provided in Appendix F.

6.7 Compressive Strength Measurement

In this study, the compression test was performed as per ASTM C469/C469M-14 [31] and ASTM C39/C39M-18 [32]. Before conducting the test, the length and weight of the cores that were stored in the laboratory for several days were recorded. Then the sulfur cap was placed at both ends of each core to provide a flat surface for applying the load. Otherwise, the load would apply on the rough surface as point loads rather than uniform load and cause premature failure.

The sample was placed in the compression test machine (SATEC Systems, Inc.). The test was performed by applying the load with a rate of 35 psi/s. The system was set up such that it stopped the load application after the peak load was achieved. Therefore, the tested core could be used for the remaining laboratory tests such as ASR detection and chloride ion penetration tests. The set-up of this test is shown in Figure 6.3. Because the length to diameter ratio of the extracted cores was less than 2:1, the correction factor was applied to the results based on ASTM C39/39M-18 [32]. In addition, the fracture pattern of each tested sample was approximated as per this ASTM.

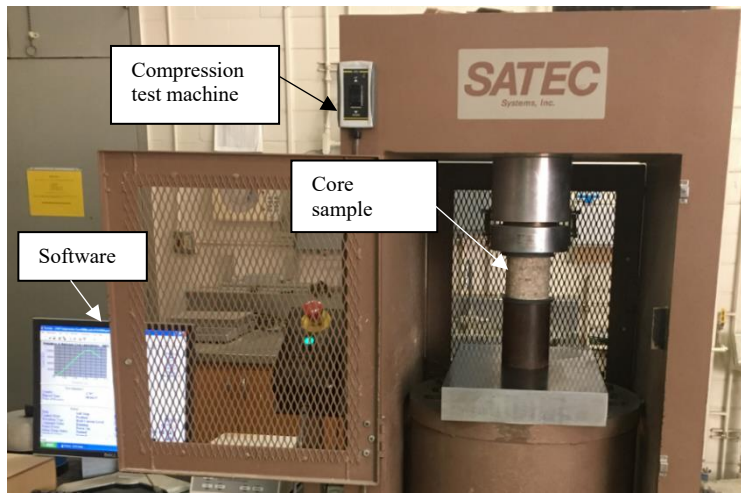


Figure 6.3: Compression test set-up

6.8 Alkali-Silica Reaction (ASR) Detection

This test was performed by using the ASR-Detect™ kit (i.e. I-AS-3000) of James Instruments Inc. The kit mainly included yellow reagent, pink reagent, distilled water, and pipettes (Figure 6.4).

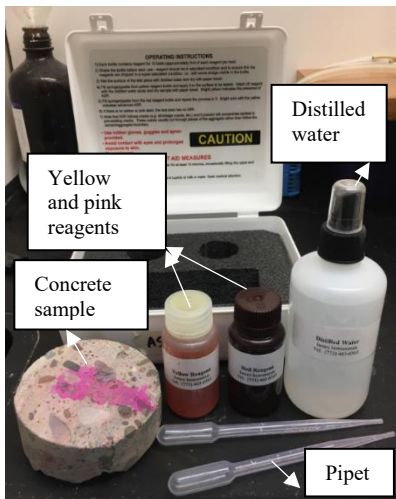


Figure 6.4: Alkali-silica reaction (ASR) detection kit

To perform the test, first distilled water was applied on the broken surface of the extracted concrete cores and dried with a paper towel. Then, the reagent bottles were shaken well to be in the saturated condition and the yellow solution was applied to the washed surface such that it covered the area of interest. After about 5 minutes the reagent was washed off with distilled water and dried the sample with a paper towel. At this step, the existence of yellow stains shows the presence of ASR reaction at the beginning stages of ASR degradation. The same procedure was performed with the pink reagent on the same area of the extracted cores tested above. The presence of both yellow and pink gels shows the beginning and advanced stages of ASR respectively. It is worth noting that the stains should be mostly around the aggregates, not the ones that appear in the cement paste. A sample for ASR gel detection procedure is shown in Figure 6.5.

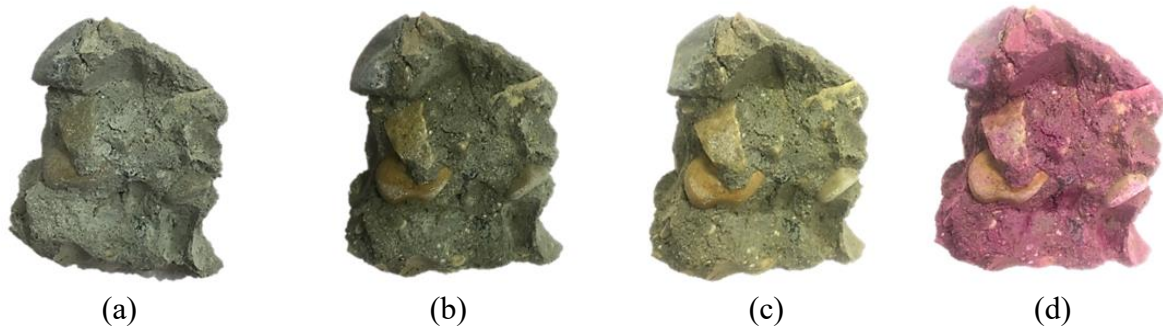


Figure 6.5: A sample of ASR gel detection procedure on SER extracted core: a) freshly cut surface, b) after application of distilled water, c) after application of yellow reagent, d) after application of pink reagent

6.9 CT Scan Imaging

In this study, the ZEISS METROTOM 800 unit was used to scan the extracted concrete cores from the visited barriers. After initializing the unit, detector calibration, geometric and axis qualification were checked to ensure they were updated recently. Otherwise, the calibration was performed to get the images with higher quality. Then, the sample was placed on the workpiece pallet in the unit, closed the loading door, and adjust the software (i.e. METROTOM OS) settings based on the size of the sample to begin scanning.

In this test, due to the high density of concrete samples, a copper filter (i.e. Cu 1 mm thickness) was placed at the outlet of the x-ray tube to reduce artifacts and increase the measuring accuracy.

Chapter 7 Field Inspections – Summary of Results and Discussion

7.1 Introduction

In this chapter, a summary of the results from field inspections of the visited barriers is presented and discussed. These include results from visual inspections (VI), half-cell potential (HCP), ground penetrating radar (GPR), and ultrasonic pulse velocity (UPV) measurements. A detailed discussion of the results in addition to the data collected for each site is provided in Appendix G.

7.2 Summary and Discussion

7.2.1 Visual Inspection

Table 7-1 shows a summary of the distress and deterioration observed in the barriers inspected. Photographs of the typical crack patterns observed at each site are shown in Figure 7.1 (more photos and distress descriptions of barriers visited are presented in Appendix G).

Site NW-1 was in good condition while site SE-2 which was built only a year earlier was severely cracked and in the worst condition among all the visited sites. Sites SE-1 and SW-1 were not in as good a condition as site NW-1 but were not as severely distressed as site SE-2 either. It is noted that site SE-1, had two segments separated by a construction joint, a west (W) and east (E) segment. Each barrier was ranked according to its condition from best to worst as shown in Table 7-2, while this ranking is somewhat subjective, it will help later comparison and discussion of the performance of the barriers.

In addition, by comparing the measured vertical crack spacing and width (Table 7-1) with the calculated values shown in Table 7-3 (details of the calculations are in section B.3 of Appendix B), it can be seen that vertical cracks were spaced at larger intervals at sites NW-1, SE-1 (W), and SW-1. This spacing was measured to be less than the expected value at sites SE-1 (E) and SE-2. Observed crack width at mid-height of barriers at all visited sites was larger than the calculated maximum crack width (see Table 7-3).

Furthermore, to provide a perspective on the level of distress along the barriers visited at each site, Table 7-4 shows the approximate percentage (per inspected length) of the good and poor condition of the barrier.

Table 7-1: Summary of observed distress and deterioration in inspected barriers

Site ID	Year of construction	The average spacing of vertical cracks (ft)	Approximate measured crack width range at mid-height of barrier (in)	Presence of horizontal cracks (Yes/No)	Map cracking observed (Yes/No)	Spalls (Yes/No)	Rust stains (Yes/No)
NW-1	2013	3 - 4	< 1/16	No	No	No	No
SE-1(W)	2015	>2	< 1/10	No	No	No	No
SE-1(E)	2015	< 2	< 1/8	Yes*	No	Yes	No
SE-2	2012	< 2	< 1/6	Yes*	Yes	Yes	No
SW-1	2014	~2	< 1/6	No	No	Yes	No

*When present horizontal cracks approximately coincide with the actual rebar location

Table 7-2: Barrier ranking based on the observed condition the field

Rank (1: best condition, 5: worst condition)	Site
1	NW-1
2	SE-1(W)
3	SW-1
4	SE-1(E)
5	SE-2

Table 7-3: Calculated average crack spacing and crack widths

Barrier type	Average crack spacing (in)	Most probable maximum crack width on the surface (in)*
S32	20	0.018-0.027
S42	21	0.017-0.026

* Crack widths shown were computed assuming uncoated (black) bars. For epoxy-coated reinforcement, as used in the barriers investigated, crack widths can be twice as wide.

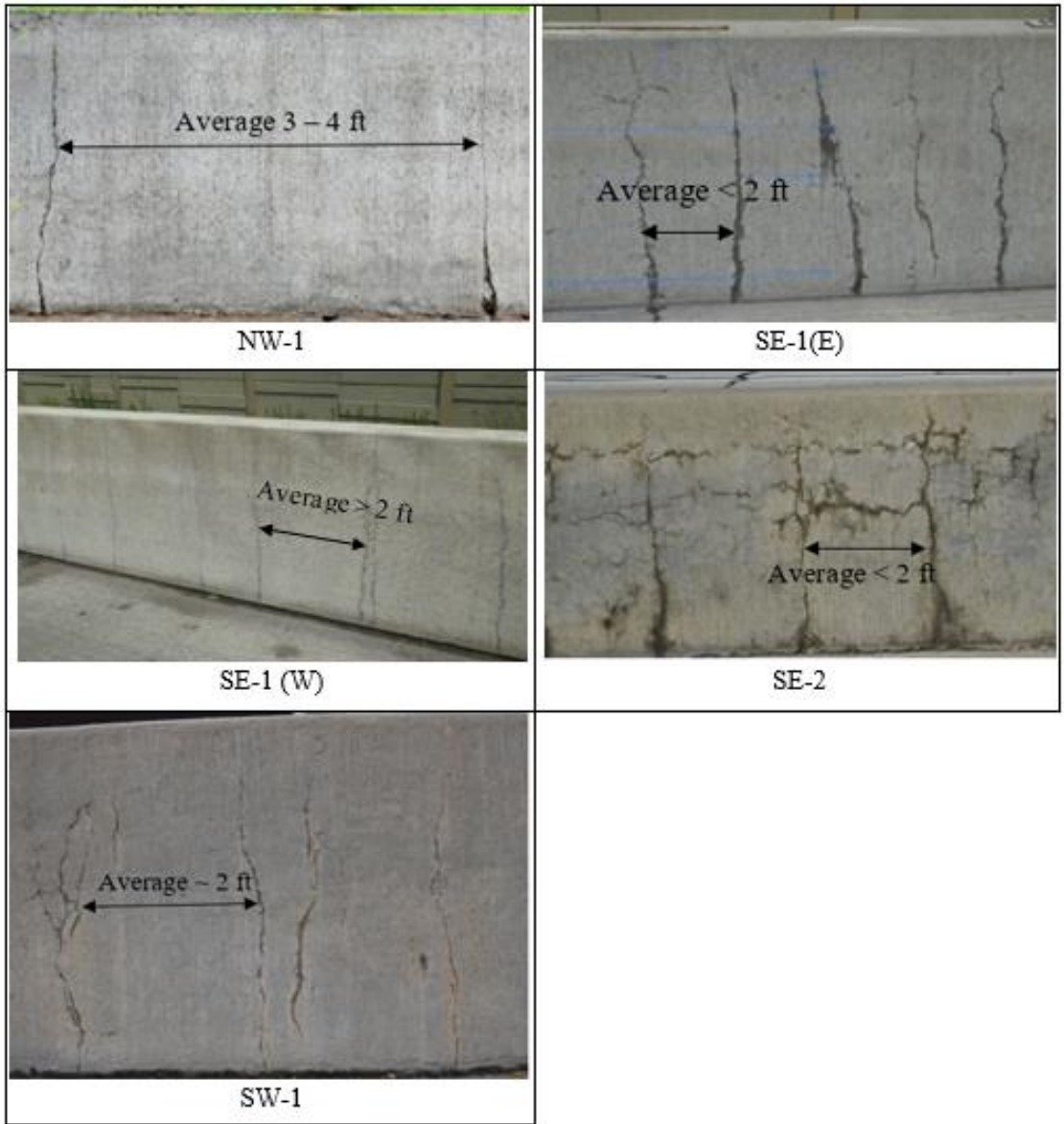


Figure 7.1: Typical crack patterns observed at each site

Table 7-4: Length and condition of barrier visited

Site ID	Inspected length (ft)	Approximate % of good condition ⁺	Approximate % of poor condition ⁺
NW-1	165	100	0
SE-1(W)	250	100	0
SE-1(E)	250	0	100
SE-2	250	0	100
SW-1	500	50	50

⁺The percentage is per inspected length.

7.2.2 Half-Cell Potential (HCP) Measurements

All barriers examined in this study were reinforced with epoxy-coated reinforcing bars. It is well known that epoxy coating is very effective at protecting steel reinforcing bars from corrosion. However, the presence of holidays due to manufacturing, or blisters created during transportation and handling of the bars in the field are a potential source of corrosion. Furthermore, vehicular barriers are probably exposed to the largest amounts of chloride-ions due to the constant spray of the passing vehicles and the accumulation of snow combined with deicing salts deposited by snowplow trucks.

To detect the likelihood of corrosion activity in the barriers, half-cell potential measurements were taken in each as described in section 5.5. Profiles of half-cell potential readings obtained at various locations along the length of the barriers are shown in Figure 7.2. As can be seen, the potential readings vary, but they do not show large drops (greater than 100 mV) along the inspected lengths. This result suggests that there is a low probability of or simply no corrosion activity in any of the barriers. This result is consistent with the absence of rust stains on the surface of the barriers (Table 7-1). Therefore, it is concluded that corrosion was not a source of deterioration of the inspected barriers.

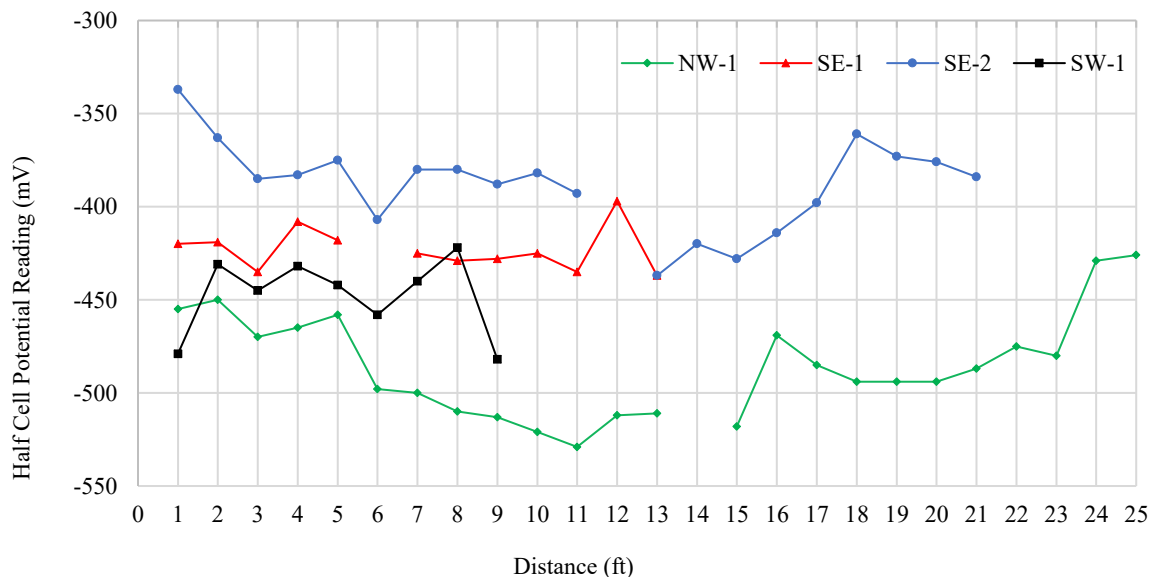


Figure 7.2: Half-cell potential readings along one longitudinal rebar at each site

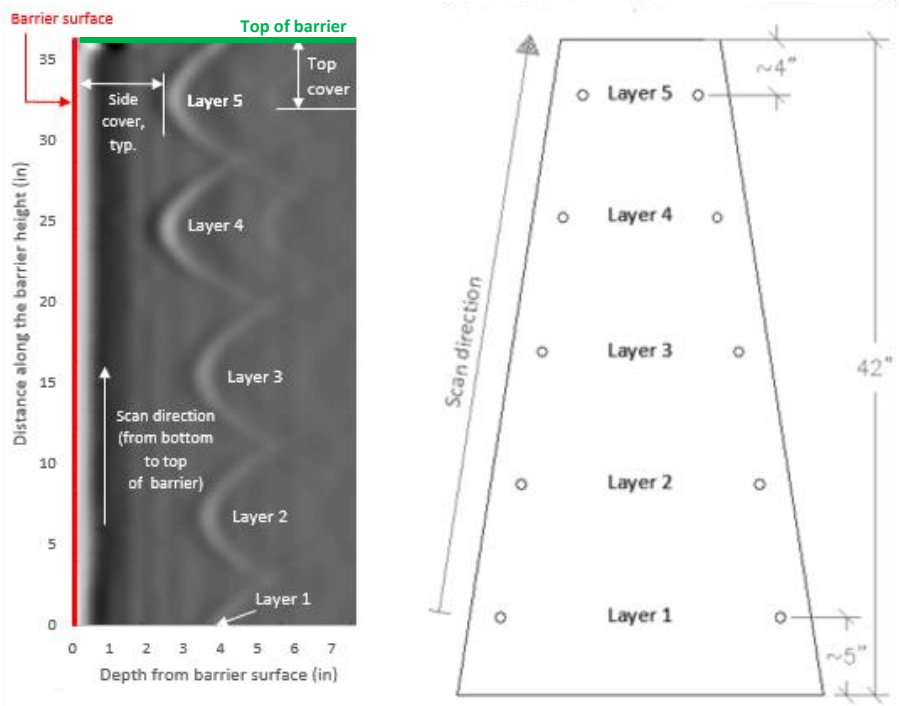
7.2.3 Ground penetrating radar (GPR)

Data from GPR show that concrete covers (i.e. top and side covers) and rebar spacing deviated (significantly in some cases) from the specified values in all barriers. Typical GPR scans with the corresponding rebar layout of two visited barriers are shown in Figure 7.3. Additional information, as well as the data collected at each site, can be found in Appendix G.

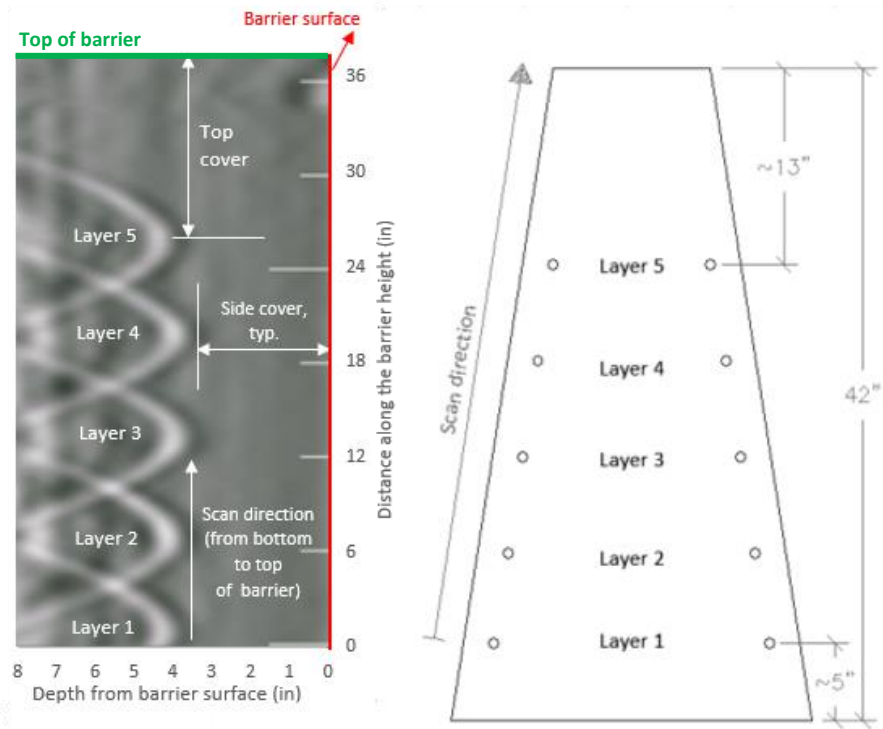
The average measured side cover at each site is shown in Figure 7.4. It can be seen that the actual bar cover is almost two times the specified value in most visited sites. This larger than specified concrete cover may be in part responsible for wider cracks on the barrier surface. The average measured rebar spacing at each site is shown in Figure 7.5. As shown in the figure, the average rebar spacing in all barriers was less than the specified value, particularly in sites SE-1 and SE-2.

While a smaller rebar spacing will generally improve crack control, the reduced bar spacing resulted in a very large “cover” at the top of the barriers at sites SE-1 (East and West) and SE-2. The top cover in the barriers at sites NW-1 and SE-1(W) can be visualized in Figure 7.3. The measured values for the top cover in all barriers in shown in Table 7-5. As shown in the table, the top layer of reinforcement was at 12 inches or more in site SE-1 and 7 inches in site SE-2, leaving a large area at the top of these barriers essentially unreinforced. The rebar layout and detail for the geometry of each barrier are presented in Appendix G.

Furthermore, GPR scan images at the barrier terminal end at site NW-1 show the existence of no vertical rebars. However, number 4 stirrups are specified within around 30 inches from the terminal ends of the barrier in the as-built drawings.



(a)



(b)

Figure 7.3: Gray scale image of vertical GPR scans obtained along the barrier height: a) site NW-1 and b) site SE-1(W)

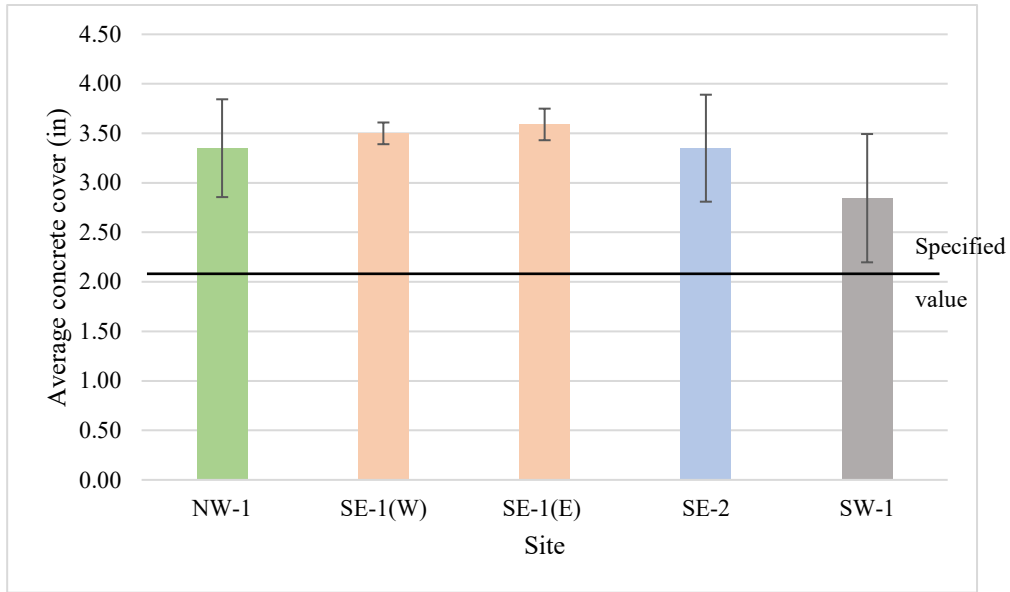


Figure 7.4: Average measured side concrete cover at different sites based on the GPR data

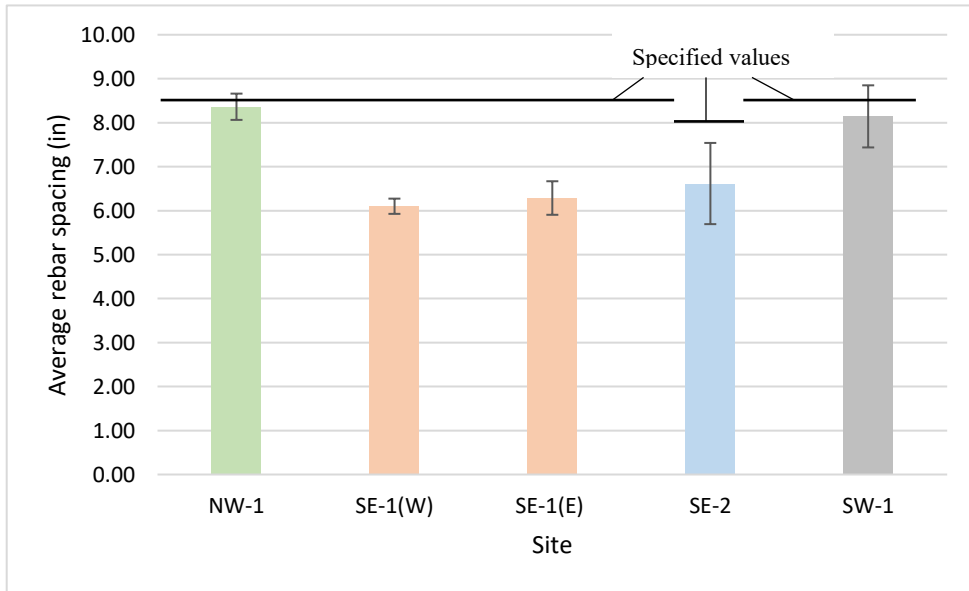


Figure 7.5: Average measured rebar spacing at different sites based on the GPR data

Table 7-5: Measured cover of the top layer of reinforcement

Site	Barrier height (in)	Top cover (in)	
		Average measured ⁺	Specified
NW-1	42	4.0	3.0
SE-1 (W)	42	13.0	3.0
SE-1 (E)	42	12.0	3.0
SE-2	32	7.0	3.0
SW-1	42	4.5	3.0

⁺ For each barrier the average of 3 locations is computed. All the measured values are within ½ of an inch from the average value.

7.2.4 Ultrasonic Pulse Velocity (UPV)

UPV measurements at site NW-1 and SW-1 were between 3500 to 6200 m/s which suggested that the concrete quality was very good to excellent [33] with no indications of large voids in these barriers. This agrees with the results of visual inspection. Data collected from the UPV tests and more discussions are provided in section G.2.4 in Appendix G.

As mentioned in Chapter 5, instrumentation malfunction prevented UPV measurements for sites SE-1 and SE-2. However, the core extraction was performed at all sites and the UPV test was conducted on the extracted cores to evaluate the quality of concrete at the visited sites in the SE region. The result is provided in Chapter 8.

Chapter 8 Laboratory Tests - Summary of Results and Discussion

8.1 Introduction

In this chapter, a summary of the results of laboratory tests on the extracted core samples is presented and discussed. The tests include core examination, carbonation depth, water absorption, UPV measurements, chloride ion penetration measurements, compressive strength, alkali-silica reaction (ASR) detection, and CT scan imaging. A detailed version of the results in addition to the collected data is provided in Appendix H.

8.2 Summary and Discussion

8.2.1 Coarse Aggregate Size and Distribution

Visual observation and CT scan images of the extracted cores mainly show the difference in the aggregate type, size, and distribution among the visited sites. The barrier at site NW-1 which was least distressed has mostly crushed aggregates with the smallest aggregate size range, while barrier segments visited at sites SE and SW regions have round shape aggregates with a large aggregate size range (Table 8-1 and Figure 8.1). These observations are consistent among all the extracted cores.

In addition, to quantify the distribution of coarse aggregates (i.e. 1 inch and larger), the area of these aggregates is calculated at a cut section of the cores using ImageJ software and divided by the core cross-section area. The results show that site NW-1 has a more uniform distribution and size of coarse aggregates compared with site SE-2. In other words, the ratio of coarse aggregates area over the core cross-sectional area is almost 12 times at site SE-2 compared with NW-1 (Table 8-2). Also, examining the extracted cores reveals no sign of honeycombing on the NW-1 core surface. However, SE-2 cores show the existence of honeycombing and poor consolidation and concrete quality. Figure 8.2 presents a sample of this observation. A detailed description of the cores with images is provided in Appendix I.

Furthermore, CT scan images show that aggregates size at site SE-1 passes the specified range, i.e. < 2 inches. A sample of this observation is shown in Figure 8.3.

Table 8-1: Cross-section of the extracted cores

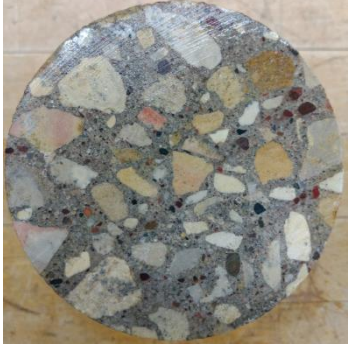

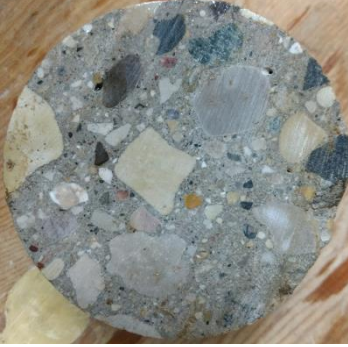

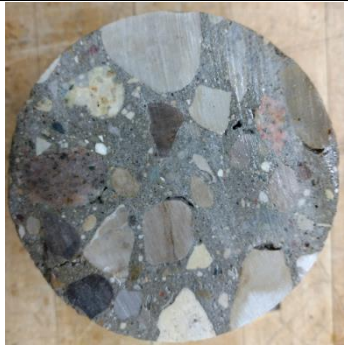
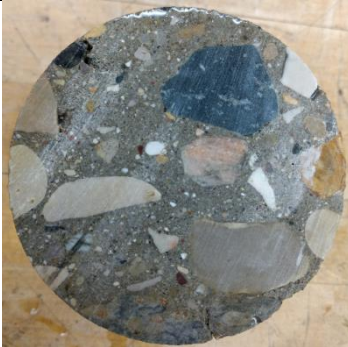




		
NW-1 (core 1)	NW-1 (core 2)	SE-1 (core 1)
		
SE-1 (core 2)	SE-2 (core 2)	SE-2 (core 3)
		
SE-2 (core 4)	SW-1 (core 1)	SW-1 (core 2)
	Note: core 1 at site SE-2 was broken, therefore there is no recorded cross-section image.	
SW-1 (core 3)		

Table 8-2: Visual appearance of the barrier vs the average large aggregate distribution at one cross-section of extracted cores and aggregate type

Site	Rank (1: best condition, 5: worst condition) (section 7.2)	Ratio of coarse aggregates area/core cross-section * 100 (%)	Aggregate type as per visual inspection of the cores
NW-1	1	1.35	Mostly Crushed
SE-1(W)*	2	4.37	Crushed + Round Gravel
SW-1	3	15.85	Crushed + Round Gravel
SE-1(E)*	4	9.81	Crushed + Round Gravel
SE-2	5	16.09	Mostly Round Gravel

*At site SE-1, west (W) and east (E) segments were in different distressed conditions.

+Coarse aggregate in this analysis was considered 1 inch and larger.

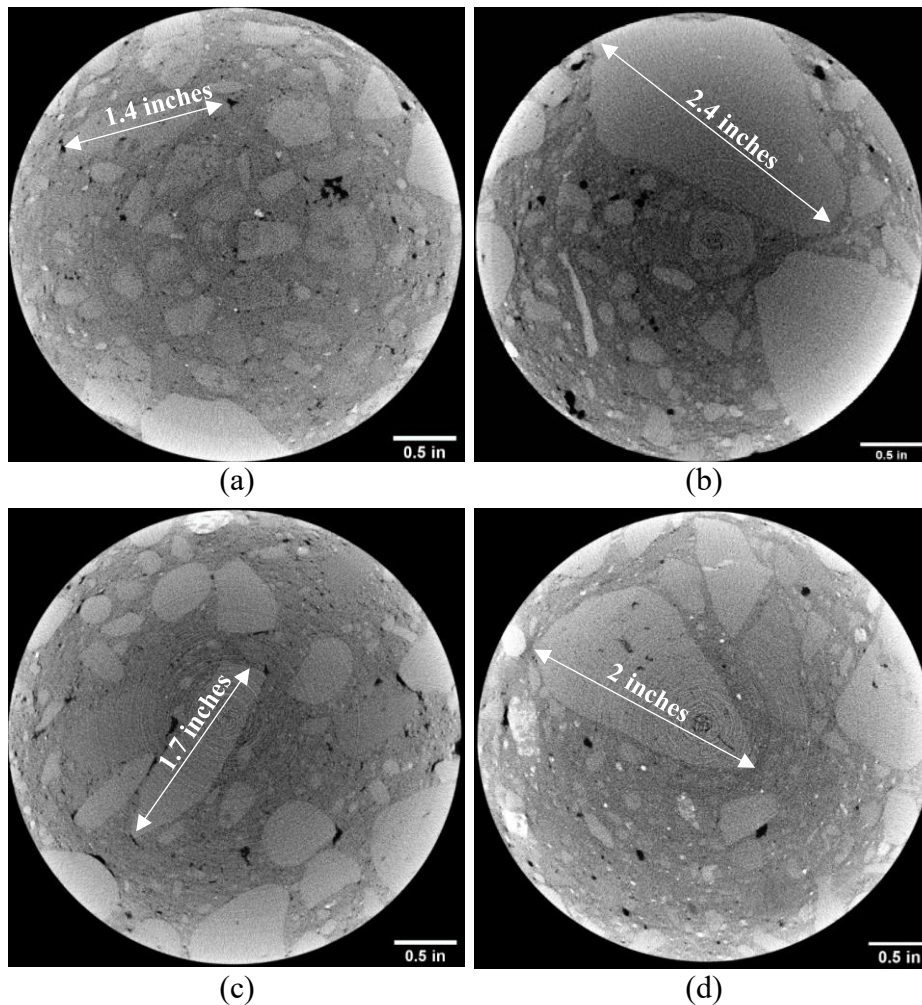


Figure 8.1: Samples of CT scan images of each site: a) site NW-1, b) site SE-1, c) site SE-2, d) site SW-1

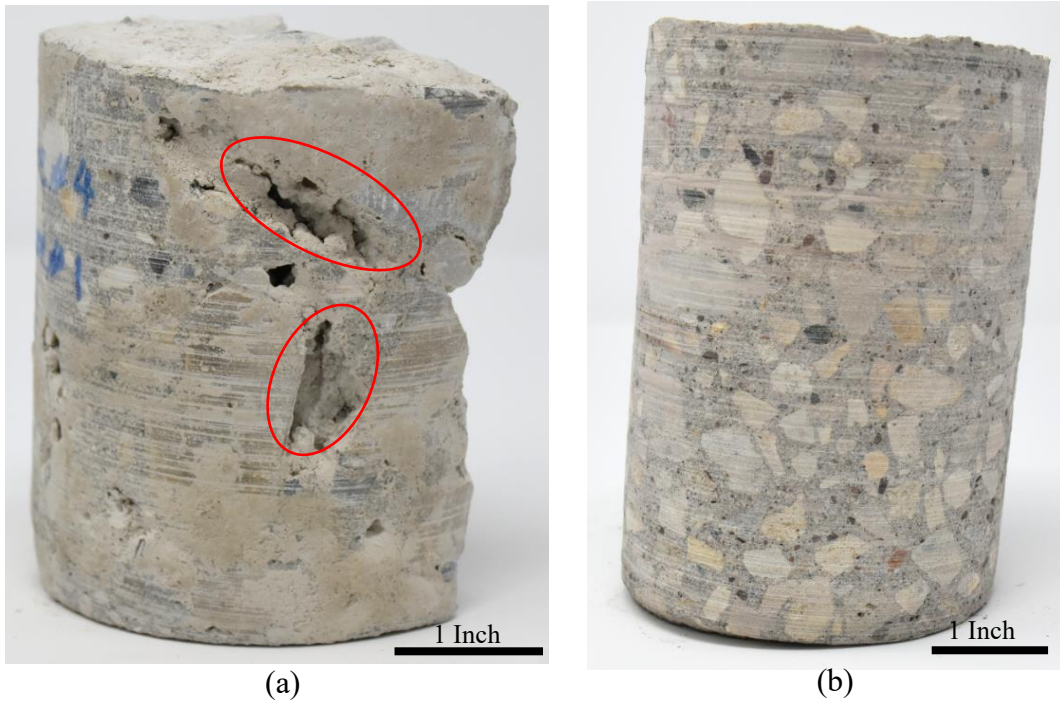


Figure 8.2: Level of honeycombing in the extracted cores: a) SE-2 (the most distressed barrier), b) NW-1 (the least distressed barrier)

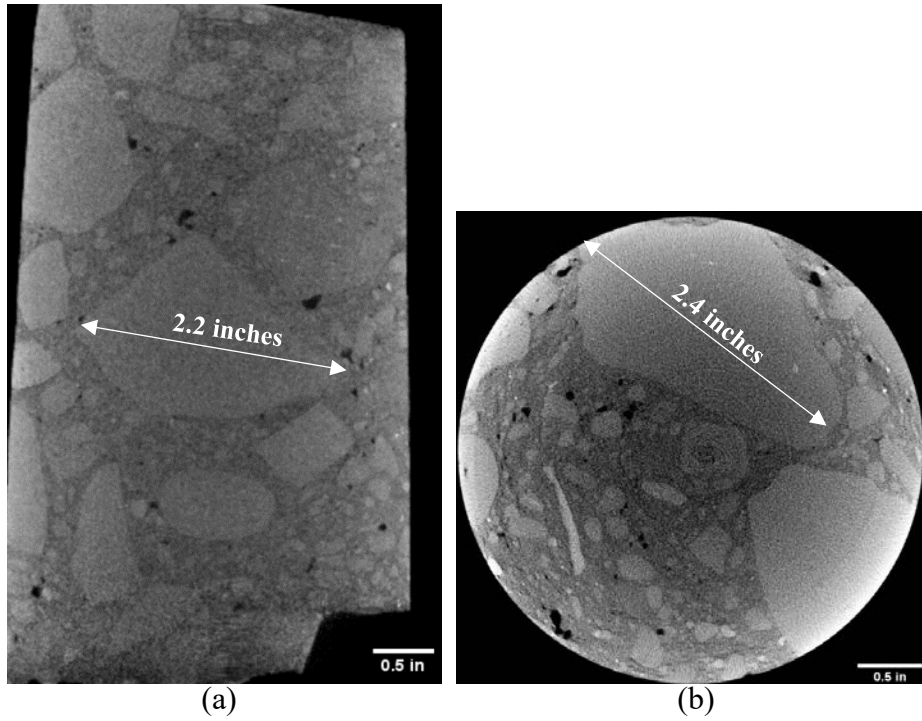


Figure 8.3: Coarse aggregate greater than the specified dimension at site SE-1: a) longitudinal view, b) cross-section view

8.2.2 Carbonation Depth

As explained in section 6.3, the carbonation depth value, d_k , was measured instantly and 24 hours after spraying the phenolphthalein solution on each broken surface of the extracted cores. The average measured carbonation depth was almost 0.08 inches in all cases. This value is significantly smaller than the rebar concrete cover (~ 4 inches). Thus, carbonation is not the main contributor to the observed distress of the barriers. The measured value for each core is presented in section H.3 in Appendix H.

8.2.3 Water Absorption

The water absorption test performed in this study does not show a considerable difference (i.e. < 5%) of the volume of permeable pore space among the sites (Figure 8.4). Therefore, based on this test, it could not be concluded that the percentage of voids would influence the level and severity of distress of barriers. The data collected at each stage of this test are provided in section H.4 in Appendix H, in addition to the computed bulk and apparent density of the cores.

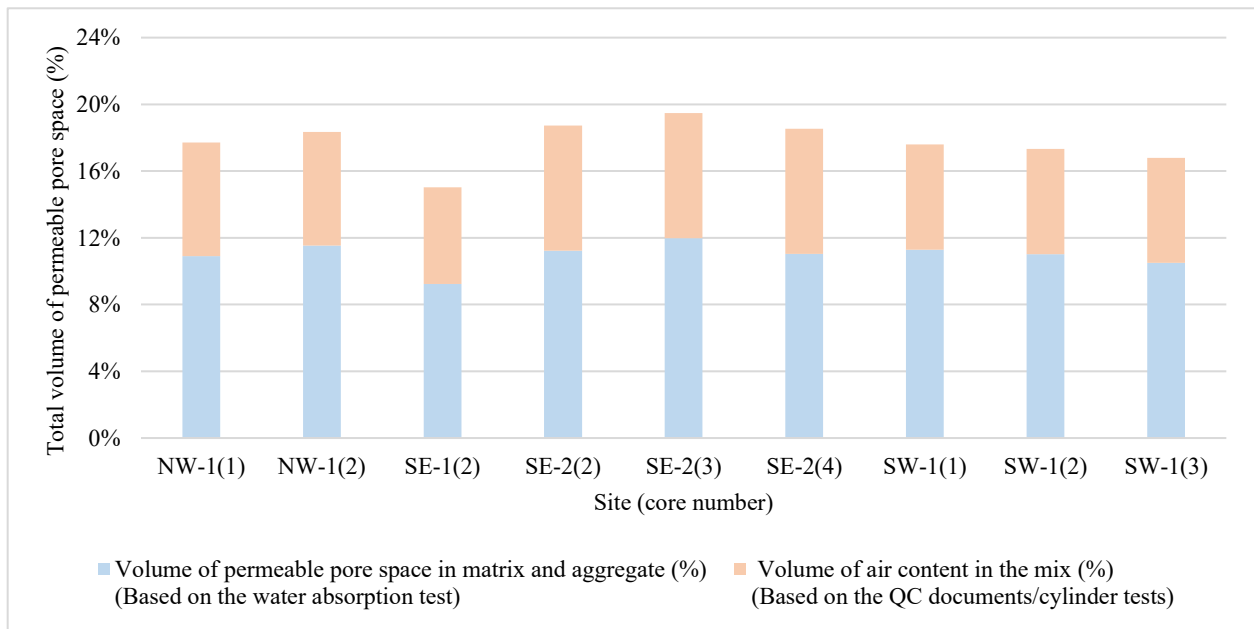


Figure 8.4: Total volume of permeable pore space (%)

8.2.4 Ultrasonic Pulse Velocity (UPV)

The results of the UPV measurements conducted on the *extracted cores* are presented in detail in Appendix H, section H.5. It may be recalled that cores were extracted from areas of the barriers in good and poor condition. However, the measured velocities for all of the cores ranged between 3500 and 4800 m/s, which correspond to concrete in good or excellent condition [33]. These results suggest that the concrete in all of the barriers was in good condition. This result is inconsistent with the actual overall condition of two of the barriers (SE-1 (E) and SE-2) and is attributed in part to the core size (diameter and length). The results of the UPV test on the extracted cores agree well with the results of UPV measurements on the barriers which were tested in the field (i.e. NW-1 and SW-1).

8.2.5 Chloride Ion Content

Since no sign of corrosion activity was identified based on visual inspection and HCP measurements, chloride ion penetration did not seem a concern. However, chloride infiltration could increase over time as cracks widen during the life span of the barrier due to freeze and thaw cycles. Thus, the analysis of the collected data from the chloride ion penetration test is provided. More discussions regarding the results of this test are provided in section H.6 of Appendix H.

The average chloride ion content measured at the surface (0.5 – 1 inch deep) at various barrier elevations is shown in Figure 8.5. As may be expected, the chloride ion content is highest in the lower part of the barrier compared with the upper portions, ranging from 3 to 7 lb/yd³. Given the large cover of the reinforcement, it was estimated that the bar-level chloride ion content was less than the threshold which could cause corrosion activity of the epoxy-coated rebars [34]. Even though chloride ion content was high, no sign of corrosion activity was observed and hence is not attributed to the distress level of the barriers.

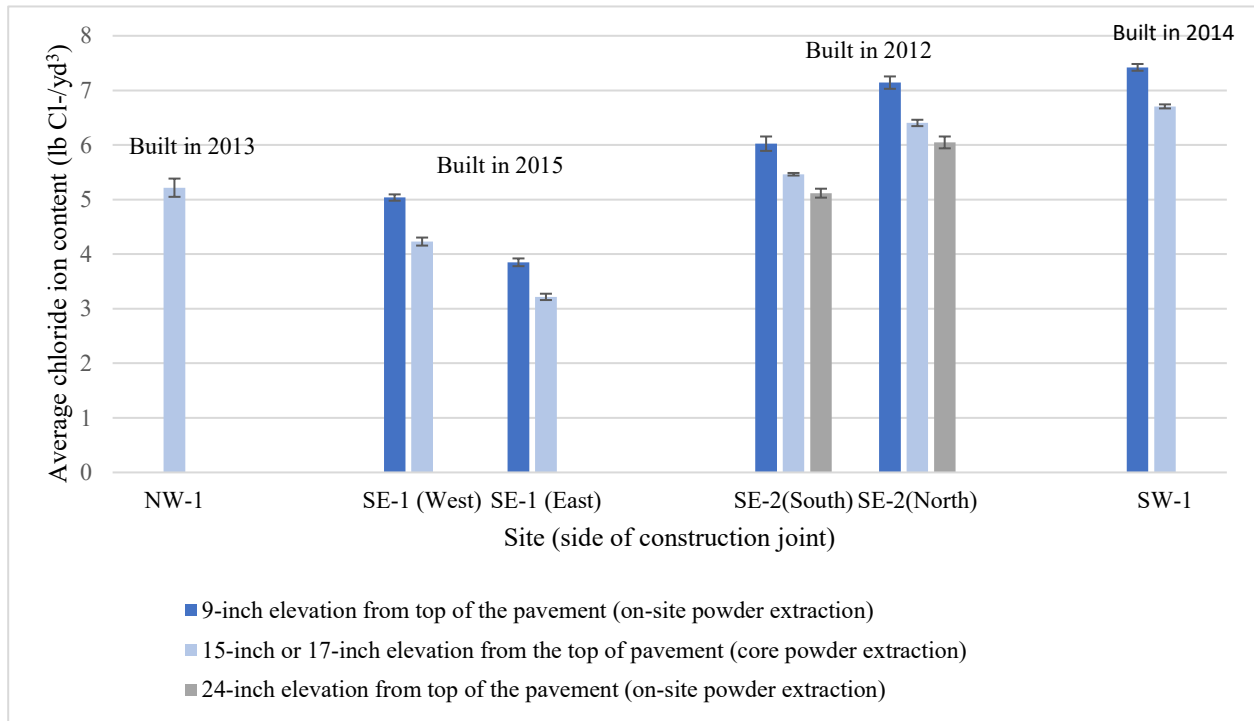


Figure 8.5: Measured chloride ion content of the extracted concrete samples at 0.5 inches to 1-inch depth (note: there was no construction joint at this sites NW-1 and SW-1)

As seen in Figure 8.5, the chloride ion content is less in the east segment than in the west segment at site SE-1. Since these two segments are exposed to the same environmental condition and they were constructed in the same year, the reason could be the difference in their concrete mix design. Reviewing the provided QC documents shows that the measured air content in the east segment was less than in the west segment (Table 8-3). Though the data are limited, this result suggests that the porosity of the latter segment could lead to higher chloride penetration.

Table 8-3: Effect of air void content on chloride ion content

Site	9-inch elevation average chloride ion content (lb. Cl-/yd³)	17-inch elevation average chloride ion content (lb. Cl-/yd³)	Measured air content in concrete mix (%) (as per QC documents)
SE-1(W)	5.04	4.23	7.3
SE-1(E)	3.85	3.22	5.8

8.2.6 Compressive Strength

Results of the compressive strength tests performed in 2020 on the cores extracted in 2019 as part of this project are compared with the cylinder test data from reports by WisDOT (Figure 8.6). By comparing the results of this test with the visual inspection ranking, it can be seen that barriers that show less deterioration have concrete with higher compressive strength. In addition, the level of deterioration increases as the compressive strength decreases (Figure 8.6). More discussions about the results of this test are provided in section H.7 of Appendix H.

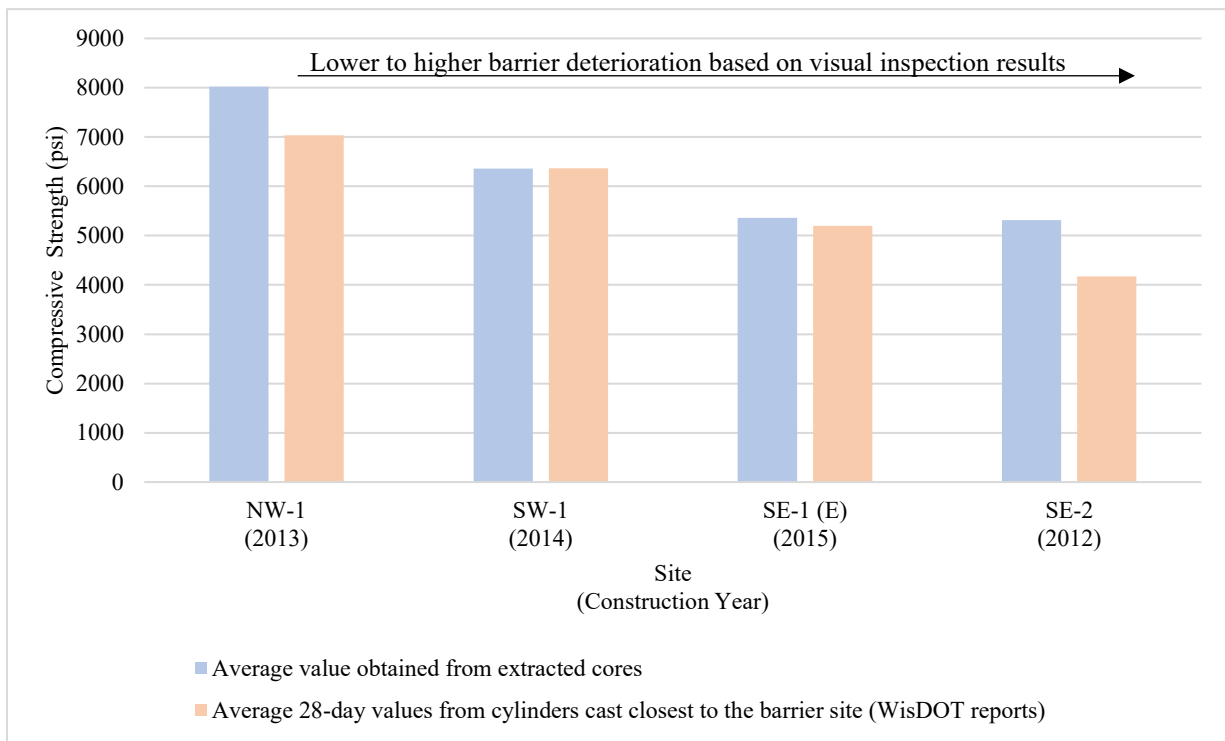


Figure 8.6: Measured compressive strength of the concrete

Chapter 9 Conclusions and Recommendations

9.1 Summary

This study was conducted to explore the main reason(s) of observed distresses such as vertical and horizontal cracks, map cracking, spalling, etc. of the single-slope slip-formed concrete barriers across Wisconsin and propose strategies and recommendations to improve the long-term performance of these barriers. The study included a state-wide survey, field measurements, and laboratory tests. The main findings discussed in the previous chapters are summarized in the following section.

9.2 Main Findings

9.2.1 Findings from the State-Wide Survey (Chapter 3)

The data gathered from this survey revealed the following:

- Vertical cracks and efflorescence were the mainly observed distress types in barriers across WI. Map cracking, spalling, and horizontal cracks although observed in some instances, were not frequently reported.
- The SE region was the one with the most reported types of distress, while the SW region had the least reported damage types.
- Most barriers are constructed during the summer except in the SE region where barrier construction during winter months was reported as well.

9.2.2 Findings from Documents Provided by WisDOT (Chapter 4)

Study of cylinder test reports and quality control documents of the closest locations to the visited barriers in addition to an investigation of specified mix design and recorded data regarding the possible aggregate source showed the following:

- Site SE-2 was the only visited site with a recorded 28-day compressive strength (i.e. as per cylinder test report) less than the specified value (i.e. less than 4500 psi).
- Sites NW-1 and SW-1 had the first and second highest recorded compressive strengths (i.e. as per cylinder test report), respectively.

- Even though all the used admixtures in the mix designs were in the approved product list of WisDOT, SE-1 and SE-2 sites had different manufacturers compared with NW-1 and SW-1 sites.
- Although the SE-1(E) site had the lowest recorded air content among sites, all the visited sites had air content within the specified range.
- The barriers at sites NW-1 and SW-1 were built in October while SE-1(W), SE-1(E), and SE-2 barriers were constructed in June, July, and September, respectively.
- Sources of aggregates (i.e. either fine or coarse) were different among all the visited sites.
- All sites had nearly the same specific gravity for either fine or coarse aggregates.
- The absorption of fine aggregates was the lowest at site NW-1 among all the visited sites. This site had the highest absorption of coarse aggregates.
- Cement type at site NW-1 was reported as type II in the cylinder test report, whereas other sites reported type I cement. The cement source of sites NW-1 and SW-1 was the same compared with the SE sites.

9.2.3 Findings from Field Inspections (Chapter 7)

The data collected from visual inspection (VI), half-cell potential (HCP) measurements, ultrasonic pulse velocity (UPV) test, and ground penetrating radar (GPR) imaging showed:

- The barrier at site NW-1 was in the best condition while the barriers at site SE-2 were severely deteriorated.
- No rust stains or other forms of corrosion activity were observed on the barrier surface. The probability of corrosion activity was measured to be very low as expected for epoxy-coated bars.
- The average measured side concrete cover was larger than the specified value at all sites. Also, the average rebar spacing was in some barriers significantly less than the specified value. Because of this reduced spacing, and most important, the barriers at sites SE-1 and SE-2 were

built with the upper layer of reinforcement with a top cover of approximately 12 inches and 7 inches, leaving the top region of the barrier unreinforced.

9.2.4 Findings from Laboratory Tests (Chapter 8)

The results gathered from carbonation depth measurement, water absorption, ultrasonic pulse velocity, chloride ion penetration, compressive strength, alkali-silica reaction (ASR) detection, and CT scan tests on the extracted cores and powder samples showed the following:

- The concrete at site NW-1 had mostly crushed aggregate with a uniform distribution of coarse aggregates. Both round and crushed aggregates were observed in the concrete at sites SE-1 and SW-1. Site SE-2 had mostly round shape aggregates with a poor distribution of coarse aggregates.
- The carbonation depth of the extracted cores was low (less than 0.08 inches).
- The total volume of permeable pore space of the concrete cores was less than a 5% difference among the cores.
- The chloride ion content at the surface ranged between 3 and 7 lb./yd³ depending on barrier elevation. However, the measured values were estimated to be less than the threshold level to induce corrosion at the bar level.
- The compression strength of concrete at site NW-1 was much higher (8000 psi) than specified (4500 psi), and was the highest among all barriers inspected in this study. Whereas, sites visited in the SE region had the lowest values of compression strength.
- CT scan images showed a significant difference between the NW cores and the other sites. The distribution of aggregate was uniform in the NW region with mostly crushed aggregate, whereas SE and SW regions had poor coarse aggregate distribution with mostly round gravels.
- ASR detection test showed no alkali-silica reactivity in the extracted cores from the visited sites.

9.3 Conclusions

It is not straightforward to identify a single explanation for the rapid deterioration observed in some of the single-slope barriers built in Wisconsin given the number of variables involved and

the limited number of barriers inspected in this study. The data collected in the field and from laboratory tests did not reveal a specific design or construction flaw that could explain observed performance. However, a few important differences in the mix design, construction, and exposure can be distinguished between the barrier that exhibited the least amount of deterioration and that with the most deterioration, as shown in Table 9-1.

Table 9-1: Summary of conclusions

Barrier in the best condition (NW-1)	Barrier in the worst condition (SE-2)
The concrete was of high quality and strength* much higher than the specified strength of 4500 psi	The concrete was of low quality and strength* lower than the specified strength of 4500 psi
Coarse aggregates are mostly no larger than ¾ inch with natural sand as fine aggregate	Coarse aggregates consisted of large size (up to 1.7 inches)
Cement Type II ⁺	Cement Type I ⁺
Horizontal reinforcement was placed within 1 inch of the specified location	Horizontal reinforcement was misplaced leaving the top ~7 inches of the barriers unreinforced
Moderate** surface-level chloride ion content (~5 lb./yd ³)	High** surface-level chloride ion content (~7 lb./yd ³)

* 28-day compressive strength of cylinders which were cast at the time of construction. These data are, geographically, the closest location to the visited segment.

+Recorded as per the cylinder test reports and concrete mix design provided by WisDOT.

** Even though chloride ion content was high, no sign of corrosion activity was observed and there is no attribution to the distress level of the barriers.

9.4 Analysis and Discussion of Results

The type of distress observed in the barriers investigated was confined primarily to the presence of vertical cracks throughout the length of the inspected segments. Minor concrete spalling along both or one of the faces of the cracks was observed over a short length in some cases. This spalling, however, was not observed to be widespread.

All barriers inspected in this study showed vertical cracks that varied in spacing, width, and length, as shown in Figure 7.1. Vertical cracks that extended over the barrier height were generally wider and extended through the thickness of the barrier. The shorter vertical cracks near the bottom do not appear to extend through the thickness, though this could not be verified in all cases because of the backfill in some of the barriers. Barrier SE-2 showed in addition horizontal cracks near the

top of the barrier as well as random cracks in all directions (map cracking) in between vertical cracks. Plausible sources of the map cracking observed in barrier SE-2 are discussed later.

If a wall (the barrier in this case) is cast on a foundation cast sometime before, shrinkage is restrained by the foundation as the early barrier concrete cools down to ambient temperatures. This gives rise to a heat-of-hydration cracking pattern consisting of large widely spaced cracks extending from the bottom to the top of the member, with some shorter vertical cracks extending from the bottom, a crack pattern that is similar to that observed in the barriers investigated in this study (Figure 7.1). Heat-of-hydration cracks can be controlled by controlling the heat rise due to heat of hydration, by placing the members in short lengths, or by providing reinforcement in excess of the normal shrinkage reinforcement [35]. It is noted that as much as three times the normal shrinkage reinforcement may be required to limit shrinkage cracks to reasonable widths [36]. The reinforcement ratio provided in barrier types S32 and S42 of this study is 0.0041 and 0.0043, respectively. This amount is about 2.2 times the standard shrinkage reinforcement. Therefore, while reinforcement in excess of the standard shrinkage reinforcement has been specified and provided in these barriers, it may not be sufficient to limit cracking to reasonable widths.

Accurate prediction of the number, size, and spacing of cracks in reinforced concrete members is, in general, a difficult task. The problem is further compounded in the case of shrinkage cracking, because of the uncertainty in predicting shrinkage strains, even under controlled environmental conditions in the laboratory. Table 7-3 shows the calculated spacing and widths of the barriers investigated. The crack spacing was estimated using the recommendations of the CEB-FIB Code [7] while the crack width was estimated using the well-known equation proposed by Gergely and Lutz [8]. The main parameters in these equations include the concrete cover, the area, and spacing of the longitudinal reinforcement, the bar diameter, the stress in the steel reinforcement, and the strain gradient. To provide a range of expected values, the spacing and crack widths were computed for steel stress of $0.67f_y$ (lower bound) and $1.0f_y$ (upper bound), where f_y is the yield stress of the reinforcement, taken as 60 ksi. Additional details of the equations and assumptions may be found in Appendix B.

The calculations show that the average spacing between vertical cracks varies slightly with barrier type, but it is expected to be about 1.7 ft. This value is in line with the observed spacing of the

large vertical cracks in all barriers, except in barrier NW-1 where the spacing of 3 to 4 ft was observed.

There are no universally agreed values of acceptable maximum crack widths. Traditionally, however, cracks wider than 0.016 in. are considered unsightly and can lead to public concern. Furthermore, cracks in exposed surfaces, as is the case of barriers, will be more noticeable due to streaks of dirt and percolated chemicals or liquids.

Other than an unsightly appearance, the observed crack widths in barriers NW-1 and SE-1 do not appear to be of concern in terms of structural integrity. On the other hand, the extent (number and size) of cracking observed in barriers SW-1 and SE-2 may be considered to affect the structural integrity of the barrier and should be avoided.

The amount of concrete cover is important to control the width of surface cracks. Many of the bars in the barriers studied were placed with a side cover much larger, up to ~ 2 times of their specified value of 2 inches. For example, with a cover of 4 inches, the crack widths shown in Table 7-3 would increase by about 20 percent. It is recognized that the standard tolerances used in common reinforced concrete construction (beams, slabs, and columns) are difficult to follow in slip-form construction of the barriers; however, every effort should be made to adhere to the specified concrete cover to control the widths of the cracks in the barriers.

As mentioned earlier, barrier SE-2 (Figure 7.1) showed map cracking in addition to vertical cracks. The most common causes for these cracks are: (a) surface drying shrinkage restrained by the underlying concrete; (b) expansion due to alkali-silica reaction (ASR); and (c) restrained thermal contraction, particularly at early ages of the concrete. Results from the ASR tests (see section 9.2.4 and Appendix H) were negative, indicating no signs of ASR in the concrete used in these barriers. Therefore, ASR is not considered a plausible source of the observed cracks in barrier SE-2 or in any of the other barriers investigated.

Map cracking due to surface drying shrinkage cracks or due to thermal expansion are nearly impossible to prevent, but they can be ameliorated by following careful construction and curing procedures. Drying shrinkage cracks can be minimized by avoiding the surface to dry before starting curing procedures; therefore, curing of the barrier should begin as soon as possible after finishing.

To control cracks due to restrained thermal contraction the temperature and heat during cement hydration must be controlled. Standard procedures to minimize concrete temperature and heat include reducing the cement content and/or cooling of the concrete. It is noted that the cement content used in barrier SE-2 was much higher (480 lbs/yd³) than the specified value for A-FA grade concrete (395 lb./yd³ [16]), which points at one of the plausible reasons for the excessive number and size of the cracks observed for this barrier.

The ambient conditions (ambient temperature, humidity, high or low winds) existing at the time of construction of the barriers investigated were not recorded and it is unknown. Also, the exact season when these barriers were constructed is not recorded. Whether standard measures to control the heat of hydration (use of insulating blankets, for example) were used in the field during construction is unknown. Therefore, it is not possible to assert whether high levels of heat of hydration contributed to the excessive cracking observed in barrier SE-2, but because of the higher cement content used in this barrier it remains as a plausible explanation.

As noted in section 7.2.1, barrier NW-1 was in a better condition than the other barriers studied. Overall, this barrier had fewer, widely spaced cracks of smaller width than those observed in the other barriers. While it is possible that appropriate field curing procedures¹ may have led to reduced cracking due to restrained shrinkage, it is noted that the 28-day concrete compressive strength used in this barrier was much higher than the specified value of 4500 psi ($f'_c \approx 7000$ psi – Table D-1 of Appendix D). In contrast, the concrete in the barrier in the worst condition (SE-2) had a 28-day compressive strength of about 4200 psi. Recognizing that the tensile (cracking) strength of the concrete is proportional to the $\sqrt{f'_c}$, the concrete tensile strength of barrier NW-1 was about $\sqrt{7000/4200} = 1.3$ times or 30% larger than that of the concrete in barrier SE-2, which can explain in part the reduced amount of cracking observed in barrier NW-1. This is important as a higher early age concrete strength will help reduce the onset of restrained shrinkage cracking.

The data from GPR and from UPV measurements taken over the inspected barrier lengths did not show indications of voids or poor consolidation to suggest widespread deterioration of stiffness or strength of the concrete. Locally, however, cores extracted from barrier SE-2 (see cores 1 and 3

¹ Curing procedures applied in the field are not actually known

for this site in Appendix I) showed evidence of voids and poor consolidation in this barrier. This is further evidence that the concrete used in this barrier was of substandard quality.

The source or type of aggregates used in the barriers, either crushed limestone or riverbed gravel, cannot be considered, per se, to influence the performance of the barriers. However, two contrasting characteristics were identified for the aggregates used in the barriers studied: size and distribution. The quality of the concrete with crushed, mostly smaller ($< \frac{3}{4}$ in) uniformly distributed gradation was in better condition than that containing large (up to 2 inches) poorly distributed coarse aggregates. Barriers in poorer condition (SE-1) had in fact what might be referred to as a gap-graded distribution with very large coarse gravel and only a few particles of smaller size aggregate. The large coarse aggregate used in barriers (SE-1) likely reduced workability and consolidation of the concrete. A more uniform gradation is expected to improve concrete strength, stiffness, workability, and long-term durability. Therefore, gap-graded, with large aggregate size (say > 1.5 inches) should be avoided.

9.5 Summary of Recommendations

- Control heat of hydration:
 - Use low heat of hydration cement or admixture to lower the heat of hydration will reduce the likelihood of developing restrained shrinkage cracks.
 - Curing should begin as soon as possible after finishing.
 - Use insulating blankets to maintain the difference between internal and external temperature to 30 F or less.
- Aggregate size/distribution use well-graded coarse aggregates with coarse aggregate size no bigger than $\frac{3}{4}$ inch. Avoid gap-graded gradation with large coarse aggregate size.
- Increasing the amount of reinforcement to about 0.005-0.0055 seems prudent. This amount corresponds to the recommended amount to control restrained shrinkage in cases of severe cracking such as those observed in barrier SE-2 [37].
- The tolerances for bar placement (spacing and concrete cover) must be tightened and every effort should be made to conform to the standard tolerances used in reinforced concrete structures.
- Data collection during and after construction should be improved. This will assist researchers in future investigations like the present study:

During construction: recording curing procedures, ambient temperature during the concreting, additional procedures followed due to cold or hot weather, slump, air content, concrete class, exact aggregate, and cement type and source for each barrier segment, aggregate gradation, aggregate properties such as specific gravity and absorption, in addition to recording separate cylinder test reports for concrete barriers (i.e. not as part of ancillary items) would be recommended. Also, documenting the concrete specified mix design which includes all the mix materials with the amount, type and manufacturer, air content, slump, and water to cement ratio would be beneficial.

After construction: performing regular inspection (yearly) to record the deterioration index with photos would help with cost analysis in future studies.

- Improving inspection and quality control during construction should ensure higher quality concrete. This could include ensuring the cement content follows the specified value (395 lb./yd³ [16]). Likewise, ensuring a sufficient number of test cylinders as per the requirement for class I concrete (provided in QMP 715) will help monitor and track the quality of the placed concrete.

References

- [1] Beason, W. Lynn, Ross, Jr, H. E., Perera, H. S., and Marek, Mark, "Single-Slope Concrete Median Barrier," *Transp. Res. Rec.*, no. 1302, 1989.
- [2] McGormley, J. C., Rende, N. S., and Krauss, P.D., "Nondestructive Evaluation and Assessment of Concrete Barriers for Defects and Corrosion," Report - Iowa Department of Transportation, BARR-010, Nov. 2013.
- [3] Henrichs, Steven R. and Luger, Matthew M., "Use of Texcote XL-70C Bridge Cote as a Concrete Surface Finish and Curing Compound," North Dakota Department of Transportation, Materials & Research Division, IM-8-029(052)065, Apr. 2009.
- [4] Staton, John F. and Knauff, Jason, "Performance of Michigan's Concrete Barriers," Michigan Department of Transportation, Lansing, MI, R-1498, Aug. 2007.
- [5] Aktan, Haluk and Attanayaka, Upul, "CAUSES & CURES FOR CRACKING OF CONCRETE BARRIERS," Center for Structural Durability, Michigan DOT Center of Excellence, RC-1448, Aug. 2004.
- [6] "Concrete Barrier Distress in La Grande, Oregon," Oregon Department of Transportation Research Unit, OR-RD-08-09, Apr. 2008.
- [7] CEB-FIB, *Model Code for Concrete Structures: CEB-FIP International Recommendations*, 3rd ed. Paris: Comite Euro-International du Beton, 1978.
- [8] P. Gergely and L. A. Lutz, "Maximum Crack Width in Reinforced Concrete Flexural Members," in *Causes, mechanism, and control of cracking in concrete*, Detroit: American Concrete Institute, 1968, pp. 87–117.
- [9] Wisconsin Department of Transportation (WisDOT), "SDD 14b32-a Concrete Barrier Single Slope-Standard, Median Retaining Wall, Anchorages." Wisconsin Department of Transportation (WisDOT).
- [10] Trierweiler Construction and Supply Co. Inc., "Concrete Cylinder Test Results - Main Project ID: 1060-33-80." Trierweiler Construction and Supply Co. Inc., 2015.
- [11] "Concrete Cylinder Test Results - Main Project ID: 1030-20-72, Test Number: 910.736 - 130 - 0363 - 2012, WisDOT." 2012.
- [12] "Concrete Cylinder Test Results - Main Project ID: 1022-08-73, Test Number 6 - 130 - 0105 - 2013, WisDOT." Nov. 2013.
- [13] "Concrete Cylinder Test Results - Main Project ID: 5300-04-77, Test Number: 1 - 130 - 0213 - 2014, WisDOT." 2014.
- [14] "Specified Concrete Mix Designs - Main Project ID: 1030-20-72." Meyer Material Company, 2010.
- [15] "State of Wisconsin Department of Transportation (WisDOT) Website." <https://wisconsindot.gov/Pages/home.aspx>.
- [16] Wisconsin Department of Transportation (WisDOT), "Section 501 Concrete." Wisconsin Department of Transportation (WisDOT), 2017.
- [17] Trierweiler Construction & Supply Co Inc, "Specified Concrete Mix Design - Main Project ID: 1060-33-80." Trierweiler Construction & Supply Co Inc, 2015.
- [18] The Aberdeen Group, "How to prevent cracks in concrete." P U B L I C A T I O N # C 6 9 0 3 4 7, 1969.
- [19] US Department of Transportation (Federal Highway Administration), "Highway Materials Engineering Course (Portland Cements)." US Department of Transportation (Federal Highway Administration).

- [20] J. R. Wright, F. Rajabipour, J. A. Laman, and A. Radlińska, “Causes of Early Age Cracking on Concrete Bridge Deck Expansion Joint Repair Sections,” *Adv. Civ. Eng.*, vol. 2014, pp. 1–10, 2014, doi: 10.1155/2014/103421.
- [21] Wisconsin Department of Transportation (WisDOT), “Section 415 Concrete Pavement.” Wisconsin Department of Transportation (WisDOT), 2017.
- [22] Wisconsin Department of Transportation (WisDOT), “Section 603 Concrete Barrier.” Wisconsin Department of Transportation (WisDOT), 2017.
- [23] Wisconsin Department of Transportation (WisDOT), “Section 716 QMP Ancillary Concrete.” Wisconsin Department of Transportation (WisDOT), 2017.
- [24] Wisconsin Department of Transportation (WisDOT), “Section 715 QMP Concrete Pavement and Structures.” Wisconsin Department of Transportation (WisDOT), 2017.
- [25] Geophysical Survey Systems Inc., “StructureScan Mini XT Manual.” Geophysical Survey Systems Inc., 2016.
- [26] Environmental Equipment + Supply, “StructureScan™ Mini HR 3D, Concrete Inspection System.” <https://www.envisupply.com/rentals/instruments/structure-scan-mini.htm>.
- [27] Cor-Map System, “C-CM-4000 Cor-Map System - Operator’s Manual.” James Instruments Inc., 2018.
- [28] ASTM International, “Standard Test Method for Detecting Delaminations in Bridge Decks Using Infrared Thermography, ASTM D4788 - 03,” 2013.
- [29] “CPC-18 Measurement of hardened concrete carbonation depth (Réunion Internationale des Laboratoires et Experts des Matériaux, systèmes de construction et ouvrages),” *RILEM Recomm. TC56-MHM Hydrocarb. Mater.*, 1988.
- [30] “Standard Test Method for Density , Absorption , and Voids in Hardened Concrete, ASTM C 642-13,” *ASTM Int.*, 2013.
- [31] “Standard Test Method for Static Modulus of Elasticity and Poisson’ s Ratio of Concrete in Compression, ASTM C469/469M-14,” *ASTM Int.*, 2020.
- [32] “Standard Test Method for Compressive Strength of Cylindrical Concrete Specimens, ASTM C39/39M - 18,” *ASTM Int.*, 2018.
- [33] Lawson, I *et al.*, “Non-Destructive Evaluation of Concrete using Ultrasonic Pulse Velocity,” *Res. J. Appl. Sci. Eng. Technol.*, vol. 3, no. 6, pp. 499–504, 2011.
- [34] Kahlaleh, Khaled Z, Vaca-cortés, Enrique, Jirsa, James O, Wheat, Harovel G, and Carrasquillo, Ramón L, “CORROSION PERFORMANCE OF EPOXY-COATED REINFORCEMENT – MACROCELL TESTS,” Texas Department of Transportation by, Research Project 1265 No. 1265-3, 1998.
- [35] A. W. Beeby and Discussion of R. I. Gilbert, “Shrinkage Cracking in Fully Restrained Concrete Members,” *ACI Struct. J. Proc.*, vol. 90, no. 1, pp. 123–126, Feb. 1993.
- [36] J. K. Wight and J. G. MacGregor, *Reinforced Concrete : Mechanics and Design*, Fifth. Pearson College Div, 2008.
- [37] R. I. Gilbert, “Shrinkage Cracking in Fully Restrained Concrete Members,” *ACI Struct. J. Am. Concr. Inst.*, vol. 89, no. 2, pp. 141–149, Apr. 1992.

Appendices

All appendices of this report which are listed in the table below are available through the link below:

<https://uwmadison.box.com/s/gl2tuiuqawcht5cwk4p674pr8p2ozcu>

Appendix	Title
Appendix A	Technical Background of Non-Destructive Evaluations and Laboratory Tests
Appendix B	Barrier Selection Criteria and Approach
Appendix C	State-Wide Survey Questions and Results
Appendix D	Description of The Inspected Barriers
Appendix E	Detailed Procedure of Field Inspections
Appendix F	Water Absorption and Chloride Ion Penetration Measurement Procedure
Appendix G	Field Inspection Data and Results
Appendix H	Laboratory Tests Data and Results
Appendix I	Detailed Core Description